



## Research paper

## Discovery of MDM2-p53 and MDM4-p53 protein-protein interactions small molecule dual inhibitors



Margarida Espadinha<sup>a,1</sup>, Elizabeth A. Lopes<sup>a,1</sup>, Vanda Marques<sup>a</sup>, Joana D. Amaral<sup>a</sup>, Daniel J.V.A. dos Santos<sup>b</sup>, Mattia Mori<sup>c</sup>, Simona Daniele<sup>d</sup>, Rebecca Piccarducci<sup>d</sup>, Elisa Zappelli<sup>d</sup>, Claudia Martini<sup>d</sup>, Cecília M.P. Rodrigues<sup>a</sup>, Maria M.M. Santos<sup>a,\*</sup>

<sup>a</sup> Research Institute for Medicines (iMed.Ulisboa), Faculty of Pharmacy, Universidade de Lisboa, Av. Prof. Gama Pinto, 1649-003, Lisboa, Portugal

<sup>b</sup> CBIOS— Research Center for Biosciences and Health Technologies, Universidade Lusófona de Humanidades e Tecnologias, 1749-024, Lisboa, Portugal

<sup>c</sup> Department of Biotechnology, Chemistry and Pharmacy, University of Siena, Via Aldo Moro 2, 53100, Siena, Italy

<sup>d</sup> Department of Pharmacy, University of Pisa, 56126, Pisa, Italy

## ARTICLE INFO

## Keywords:

Cancer  
Dual inhibitors  
MDMs  
p53  
Spiropyrazoline oxindoles

## ABSTRACT

MDM2 and MDM4 are key negative regulators of p53, an important protein involved in several cell processes (e. g. cell cycle and apoptosis). Not surprisingly, the p53 tumor suppressor function is inactivated in tumors over-expressing these two proteins. Therefore, both MDM2 and MDM4 are considered important therapeutic targets for an effective reactivation of the p53 function. Herein, we present our studies on the development of spiropyrazoline oxindole small molecules able to inhibit MDM2/4-p53 protein-protein interactions (PPIs). Twenty-seven potential spiropyrazoline oxindole dual inhibitors were prepared based on *in silico* structural optimization studies of a hit compound with MDM2 and MDM4 proteins. The antiproliferative activity of the target compounds was evaluated in cancer cell lines harboring wild-type p53 and overexpressing MDM2 and/or MDM4. The most active compounds in SJS-A-1 cells, **2q** and **3b**, induce cell death via apoptosis and control cell growth by targeting the G0/G1 cell cycle checkpoint in a concentration-dependent manner. The ability of the five most active spiropyrazoline oxindoles in dissociating p53 from MDM2 and MDM4 was analyzed by an immunoenzymatic assay. Three compounds inhibited MDM2/4-p53 PPIs with IC<sub>50</sub> values in the nM range, while one compound inhibited more selectively the MDM2-p53 PPI over the MDM4-p53 PPI. Collectively, these results show: i) **3b** may serve as a valuable lead for obtaining selective MDM2-p53 PPI inhibitors and more efficient anti-osteosarcoma agents; ii) **2a**, **2q** and **3f** may serve as valuable leads for obtaining dual MDM2/4 inhibitors and more effective p53 activators.

## 1. Introduction

Cancer is a leading cause of death worldwide and the main barrier to life expectancy increase [1]. Anticancer therapies using small molecules are still the most used in the clinic. However, one of the major limitations of these therapies is their toxicity to normal cells and tissues. Therefore, the development of targeted anticancer therapies represents a superior approach to traditional chemotherapy drugs [2]. Perturbations on the tumor suppressor protein p53 pathway are common events in carcinogenesis, making this protein one of the most relevant therapeutic targets in cancer. In tumors harboring wild-type (wt) p53, the

most studied strategy for p53 reactivation relies on inhibiting MDM2, one of the main p53 downregulators [3–9]. However, in tumors with high levels of MDM4 (also known as MDMX), another negative regulator of p53, the effectiveness of MDM2 inhibitors and their use in the clinic are compromised [10,11]. Efforts have been done to develop selective MDM4 inhibitors, as well as dual MDM2/4 inhibitors (Fig. 1), however, to date, only the stapled peptide ALRN-6924 has reached clinical trials. For these reasons, developing small molecules able to inhibit MDM4-p53 protein-protein interaction (PPI) or act as dual inhibitors of MDM2/4-p53 protein-protein interactions (PPIs) is urgently required [11,12].

\* Corresponding author. Medicinal Organic Chemistry Group, iMed.Ulisboa Faculty of Pharmacy, Universidade de Lisboa Av. Prof. Gama Pinto, 1649-003, Lisboa, Portugal.

E-mail address: [mariasantos@ff.ulisboa.pt](mailto:mariasantos@ff.ulisboa.pt) (M.M.M. Santos).

<sup>1</sup> These authors contributed equally to this work.

<https://doi.org/10.1016/j.ejmech.2022.114637>

Received 10 June 2022; Received in revised form 22 July 2022; Accepted 25 July 2022

Available online 5 August 2022

0223-5234/© 2022 Published by Elsevier Masson SAS. This is an open access article under the CC BY license (<http://creativecommons.org/licenses/by/4.0/>).

Small molecules that target MDMs usually mimic the key p53 residues involved in the p53-MDM2/4 PPIs: Trp23, Phe19, Leu26, and Leu22. Although there is a high degree of homology in the N-terminus domains of MDM2 and MDM4, dual inhibitors are challenging to design due to structural and conformational differences between the binding sites of both proteins. MDM2 binding site is more flexible and can easily adapt to the ligands, while the p53 binding site on MDM4 is more rigid and smaller [13].

Previously, we have developed spirooxindoles containing a pyrazoline ring to obtain novel small molecule p53 activators through inhibition of the p53 negative regulator MDM2 [14–16]. The pyrazoline ring allows the projection of four different groups, representing an ideal chemotype in the search for dual MDM2/4 inhibitors. Our previous studies led to the identification of hit spiropyrazoline oxindole **1** (Fig. 2) which induces cell cycle arrest and upregulates p53 steady-state levels in HCT116 cells, while decreasing MDM2 levels [15]. In this work, we optimized this hit compound in order to obtain dual MDM2/4-p53 PPIs. To achieve this goal, *in silico* studies were performed to design new series of spiropyrazoline oxindoles, which were then synthesized. The anti-proliferative activity of the novel compounds was evaluated in four wt p53 human cancer cell lines, followed by mechanistic studies with the most promising candidates.

## 2. Results and discussion

**In silico experiments.** The crystallographic structures of MDM2 and MDM4 were used to explore the binding modes of spiropyrazoline oxindole **1**. The 5-bromooxindole moiety fills the Trp23 pockets in MDM2 and MDM4 by establishing a hydrogen bond between the indole NH and the carbonyl of the <sup>MDM2</sup>Val93 and <sup>MDM4</sup>Met53 backbones, respectively. The N-phenyl ring, occupying the Leu26 pocket, establishes a  $\pi$ - $\pi$  stacking interaction with <sup>MDM2</sup>His96. This interaction does not exist between compound **1** and MDM4, due to the replacement of His96 by Pro96. The other two phenyl groups occupy the Phe19 and the Leu22 pockets, establishing mainly hydrophobic interactions with both MDM2 and MDM4 proteins (Fig. 3). Despite these interactions, spiropyrazoline oxindole **1** does not establish polar interactions in the solvent-exposed pocket (Leu22 pocket), which are essential for strong binding affinity to MDM2 and MDM4.

To enhance the affinity for MDM2 and MDM4, each substituent of hit compound **1** was modified independently and the resulted structures were docked. In the Trp23 deep pocket, small substituents can be added in different positions of the oxindole, such as halogens and small alkyl groups. The phenyl group occupying the highly hydrophobic Phe19 pocket was replaced by other alkyl and aryl groups, such as morpholine, cyclohexane, piperidine, and halogen/methoxy-substituted phenyl

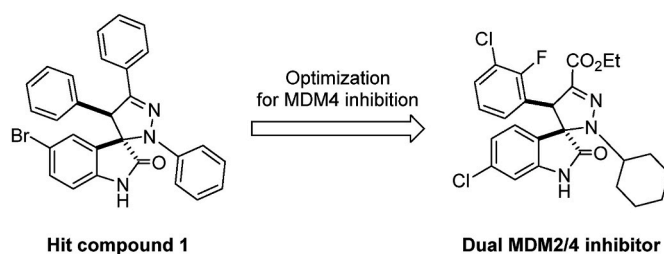


Fig. 2. Structural optimization of spiropyrazoline oxindoles as potent MDM2/4-p53 PPIs inhibitors.

rings. In the Leu26 pocket, the  $\pi$ - $\pi$  stacking interaction between the phenyl group and <sup>MDM2</sup>His96 residue is critical. For this reason, the aromatic substituent was maintained, and small group substituents (OH and halogens) were added to increase the interactions and fulfill this pocket. In the solvent-exposed pocket, the hydrophobic phenyl substituent was replaced by hydrophilic groups, such as ester, amide, heterocycles, and alcohol chains. These groups can establish hydrogen bonds with the hydrophilic residues of this pocket, as well as increase the solubility of the compounds. Based on these modifications, the compounds with higher scores for MDM2 and MDM4 were then synthesized (Fig. 4). In this first compound series, all the substituents in the pyrazoline ring occupy the same pockets in both proteins.

For the second round of optimization, we only focused on MDM4, as this protein is more difficult to target than MDM2 due to its rigidity, shape and pocket size [13]. Using as starting point the spiropyrazoline oxindole **3a**, with  $R^1 = 6\text{-Cl}$  (hydrogen bond with <sup>MDM4</sup>Met54 residue),  $R^2 = 3\text{-OH-Ph}$  (hydrogen bond with <sup>MDM4</sup>Val93 residue),  $R^3 = \text{CO}_2\text{Et}$  and  $R^4 = p\text{-Cl-Ph}$ , modifications were applied on the solvent-exposed pocket ( $R^3$ ). The OEt of the ester group was manually removed and a novel series of spiropyrazoline oxindoles, with molecular weight below 700, was built by anchoring different fragments at the carbonyl group. This library was virtually screened against MDM4 crystallographic structure and the top-ranked ligands presented an amide with hydrogen donors/acceptors and ionic groups as a common feature. The nitrogen from the amide group was used as anchoring point to construct a third series of compounds. The best-ranked compounds resulting from this screening were also able to establish additional hydrogen bonds with <sup>MDM4</sup>Tyr100, <sup>MDM4</sup>Lys94, and/or <sup>MDM4</sup>Gln72. From these two screenings, seven novel derivatives (**3b-h**) were selected to be synthesized (Fig. 5).

**Chemistry.** Spiropyrazoline oxindoles **2** and **3** were prepared using the general synthetic route presented in Scheme 1. Aldolic condensation reaction between oxindole derivatives and benzyl aldehydes gave 3-methylene indolin-2-ones **4** in 69–93% yield, using reported

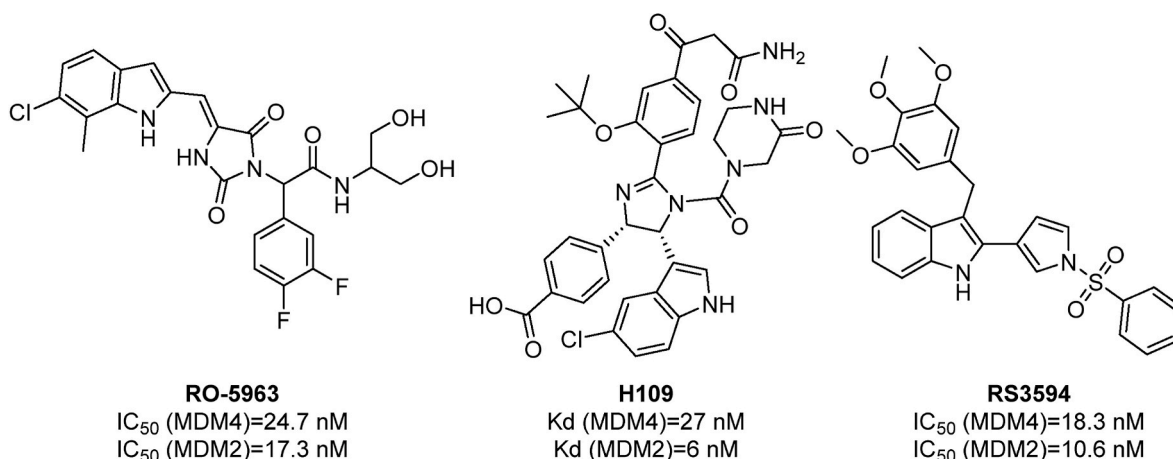
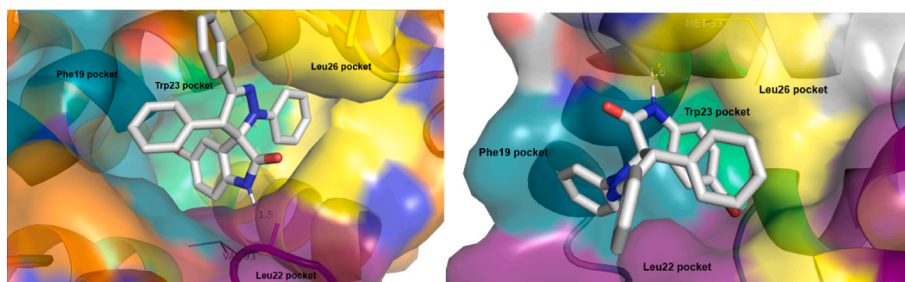
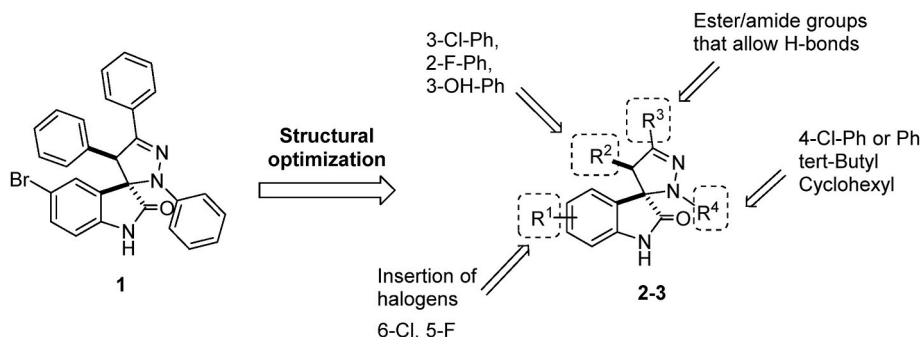


Fig. 1. Representative examples of dual MDM2/4 inhibitors.



**Fig. 3.** - Predicted binding poses between spiroprazole oxindole **1** (grey sticks) and MDM2 (PDB code 4WT2, surface and cartoon on the left) and MDM4 (PDB code 3LBJ, surface and cartoon on the right). H-bond between the oxindole moiety to <sup>MDM2</sup>Val93 and <sup>MDM4</sup>Met54 are depicted. Each color of the surface represents each pocket of the binding site (teal – Phe19 pocket, purple – Leu22 solvent-exposed pocket, green – Trp23 pocket, and yellow – Leu26 pocket).



**Fig. 4.** Structural modifications in compound **1** leading to the first series of spiroprazole oxindoles.

conditions [17]. Hydrazonyl chlorides **5** were obtained in high yield (83–96%) by reaction of hydrazines with ethyl 2-oxoacetate, followed by chlorination of the resulting hydrazones with *N*-chlorosuccinimide [18]. Synthetic procedures and characterization of intermediates **4** and **5** can be found in SI.

A synthetic optimization was carried out first to obtain spiroprazole oxindoles containing an ethyl ester group at position 5'. We tested different solvents (dichloromethane, tetrahydrofuran, acetonitrile, and toluene), temperature (room temperature and reflux), reaction time (15–96 h), and stoichiometry of reagents to obtain compound **2a** (Table 1). Using conditions previously reported by our group, no reaction was observed between 3-methylene indolin-2-one **4a** and hydrazonyl chloride **5a** in the presence of triethylamine at room temperature (Entry 1, Table 1) [14]. Higher temperatures led to the formation of spiroprazole oxindole **2a** in 55–95% yields (Entries 2–5, Table 1). The highest yield was obtained after 96 h of reaction using acetonitrile as solvent. To improve the reaction time, the 1,3-dipolar cycloaddition was tested in a sealed tube at 90 °C, using acetonitrile as solvent. Under pressure conditions, the reaction time decreased to 15 h, while maintaining a good yield of **2a** (Entry 6 versus Entry 4, Table 1). A decrease in the number of equivalents of hydrazonyl chloride from 2.0 to 1.5 equivalents (Entries 7–9 versus Entry 6, Table 1) together with the use of 3.0 equivalents of triethylamine revealed to be the best conditions to obtain spiroprazole oxindole **2a** (89% yield, Entry 8, Table 1). In addition, increasing the reaction time from 15 h to 24 h did not improve the reaction outcome (Entry 8 versus Entry 9, Table 1).

The best reaction conditions (acetonitrile, sealed tube, 90 °C, 1.5 eq. of hydrazonyl chloride and 3.0 eq. of triethylamine, Entry 8, Table 1) were applied to the synthesis of spiroprazole oxindoles **2c**, **2h-s** and **3a** (11–90% yield). The carboxylic acid derivatives **2b** and **2d** were prepared through hydrolysis of derivatives **2a** and **2c** in the presence of sodium hydroxide (92–97% yield). Amide derivatives **2e-g** were obtained by HOBt/TBTU-mediated amide coupling of the carboxylic acid derivative **2d** with the respective primary amines (42–46% yield). Amide derivatives **3b-h** were prepared by hydrolysis of derivative **3a**

with lithium hydroxide followed by amide couplings (40–70% yield) (Scheme 1 and Table 2).

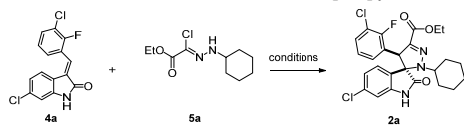
*In vitro* antiproliferative assays in wt p53 cancer cells and SAR analysis. The antiproliferative potential of spiroprazole oxindoles **2a-s** and **3a-h** was first evaluated in wt p53 HCT116 human colon cancer cell line that overexpresses MDM2. The determined IC<sub>50</sub> values are presented in Table 2.

Derivatives with 6-chloro or 6-chloro-5-fluoro substituents in the oxindole moiety had comparable IC<sub>50</sub> values (**2c** versus **2r** and **2m** versus **2s**). In addition, the presence of halogens in *meta* position (R<sup>2</sup>) of the phenyl ring (**2h**, IC<sub>50</sub> = 25.5 μM and **2l**, IC<sub>50</sub> = 27.5 μM) promoted an increase in potency compared to halogens in *para* position (**2j**, IC<sub>50</sub> = 39.1 μM and **2o**, IC<sub>50</sub> = 31.7 μM). Also, the introduction of an *ortho*-fluoro group did not result in higher potency (**2a**, IC<sub>50</sub> = 23.6 μM versus **2h**, IC<sub>50</sub> = 25.5 μM). Four different groups were tested at R<sup>4</sup>: *tert*-butyl, cyclohexyl, phenyl, and 4-chloro-phenyl. The higher antiproliferative activity was obtained when R<sup>4</sup> was replaced from cyclohexyl (**2a**, IC<sub>50</sub> = 23.6 μM), *tert*-butyl (**2c**, IC<sub>50</sub> = 32.1 μM) or phenyl (**2n**, IC<sub>50</sub> = 29.9 μM) groups by a 4-chloro phenyl group (**2q**, IC<sub>50</sub> = 18.0 μM). Carboxylic acid derivatives **2b** and **2d** did not show any antiproliferative activity in HCT116 cells (IC<sub>50</sub> > 100 μM). Amide derivatives **2e-g** had comparable or lower antiproliferative effect than the corresponding ester derivative **2c**. Spiroprazole oxindole **2e**, with a similar size chain of ester **2c**, was not active at the tested concentrations. For derivatives with bulkier and longer chains there were no differences in the cell response (**2f-g** versus **2c**, Table 2).

From the second round of optimization (**3b-h**), derivatives containing a 3-hydroxyphenyl ring at R<sup>2</sup>, the most potent compounds were spiroprazole oxindoles **3b** and **3f** with IC<sub>50</sub> values of 18.8 and 20.9 μM, respectively.

Both derivatives contain a phenyl linked to the pyrazole ring as amide substituent, with derivative **3f** having an additional phenyl ring linked to the pyrazole moiety. Moreover, there was no significant difference in activity between a 4-aminophenol (**3c**, IC<sub>50</sub> = 27.2 μM) and 4-(2-aminoethyl)phenol (**3d**, IC<sub>50</sub> = 27.0 μM) substituents. In general,



**Table 1**Optimization of the reaction conditions to obtain spiropyrazoline oxindole **2a**.

Entry <sup>a</sup>	4a (eq.)	5a (eq.)	Et <sub>3</sub> N (eq.)	Time (h)	Solvent	T (°C)	Yield (%)
1	1	2	2	96	CH <sub>2</sub> Cl <sub>2</sub>	r.t.	–
2	1	2	2	96	CH <sub>2</sub> Cl <sub>2</sub>	reflux	70
3	1	2	2	96	THF	reflux	82
4	1	2	2	96	MeCN	reflux	95
5	1	2	2	96	Toluene	reflux	55
6	1	2	2	15	MeCN	90	85
7	1	1.5	1.5	15	MeCN	90	36
8	1	1.5	3	15	MeCN	90	89
9	1	1.5	3	24	MeCN	90	89

<sup>a</sup> The reactions in entries 6–9 were performed in a sealed tube.

small substituents led to a decrease in activity compared to bulkier substituents (**3e**, **3g-h** versus **3b**, **3f**). In the case of spiropyrazoline oxindole **3h**, no dose-response effect was observed (Table 2).

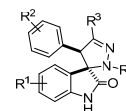
Spiropyrazoline oxindoles **2a-s** and **3a-h** were also screened at 20 μM in three other human cancer cell lines harboring wt p53 and over-expressing MDM2 and/or MDM4 (Fig. 6): osteosarcoma (SJSA-1), prostate carcinoma (LNCaP), and breast adenocarcinoma (MCF-7). In LNCaP cell line, the compounds were also tested at 10 μM, since at a concentration of 20 μM most compounds exhibited similar cell viability. A 40% cellular viability threshold was established, and compounds **2q** and **3b** presented the highest antiproliferative activity in all three cell lines tested (Fig. 6).

The IC<sub>50</sub> values for the most promising compounds (darker bars, Fig. 6) were determined (Table 3). Derivatives **2q**, **3b**, and **3f** were the most active compounds in the four wt p53 cell lines used (HCT116, SJSA-1, LNCaP, and MCF-7). Additionally, three other derivatives also showed interesting activities: **2a** in SJSA-1 cells (IC<sub>50</sub> = 12.6 μM), **2l** in LNCaP cells (IC<sub>50</sub> = 13.1 μM), and **3c** in MCF-7 cells (IC<sub>50</sub> = 14.3 μM). All the selected compounds have in common bulky groups at R<sup>3</sup> and cyclohexyl or 4-Cl-Ph groups at R<sup>4</sup>.

Compounds **2q** and **3b**, the two most promising compounds in SJSA-1, MCF-7 and LNCaP cells, with cellular viability inferior to 40%, were selected for further assays in SJSA-1 cells. This cell line was chosen since is derived from osteosarcoma, a type of cancer characterized by drug resistance and high metastatic potential [19]. As expected, both compounds significantly reduced SJSA-1 cellular viability (Fig. 7). Then, the cytotoxicity of the two compounds was evaluated in HEK293T cells, an *in vitro* model for kidney cytotoxicity [20]. No effect on HEK293T cell viability was exerted by derivative **3b** at 15 μM, while for derivative **2q** a decrease of 24% cell viability was observed at the tested concentration. Moreover, to confirm the contribution of p53 activation to compound activity in HCT116 p53<sup>(+/+)</sup> cells, **2q** and **3b** were tested in HCT 116 p53<sup>(-/-)</sup> cells in which p53 has been knocked out. Compound **2q** was selective for HCT116 p53<sup>(+/+)</sup> over the isogenic pair without p53, having only a decrease of 13% cell viability when tested at 20 μM in HCT116 p53<sup>(-/-)</sup> cells (1.1 × IC<sub>50</sub> in HCT116 p53<sup>(+/+)</sup> cells). However, a decrease of 52% cell viability was observed for compound **3b** at the tested concentration in HCT116 p53<sup>(-/-)</sup> cells, revealing that additional mechanisms, besides p53-dependent effects, may contribute for compound **3b** antiproliferative activity.

To get insights into the antiproliferative effect of compounds **2q** and **3b**, mechanistic studies were also conducted in SJSA-1 cells.

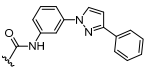
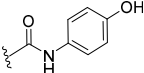
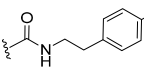
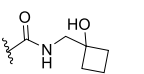
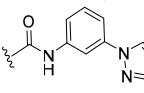
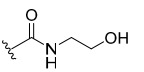
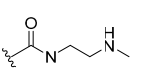
**Compounds 2q and 3b induce cell death and apoptosis in SJSA-1 cells.** Lactate dehydrogenase (LDH) release was measured in SJSA-1

**Table 2**– *In vitro* antiproliferative activities (IC<sub>50</sub>) of spiropyrazoline oxindoles **2a-s** and **3a-h** in HCT116 cells.

Compound	R <sup>1</sup>	R <sup>2</sup>	R <sup>3</sup>	R <sup>4</sup>	IC <sub>50</sub> (μM) HCT116
<b>2a</b>	6-Cl	3-Cl	CO <sub>2</sub> CH <sub>2</sub> CH <sub>3</sub>	Cyclohexyl	23.6 (95% CI) 20.7–26.9)
<b>2b</b>	6-Cl	3-Cl	CO <sub>2</sub> H	Cyclohexyl	>100
<b>2c</b>	6-Cl	3-Cl	CO <sub>2</sub> CH <sub>2</sub> CH <sub>3</sub>	<i>tert</i> -Bu	32.1 (95% CI) 28.8–35.8)
<b>2d</b>	6-Cl	3-Cl	CO <sub>2</sub> H	<i>tert</i> -Bu	>100
<b>2e</b>	6-Cl	3-Cl		<i>tert</i> -Bu	>50
<b>2f</b>	6-Cl	3-Cl		<i>tert</i> -Bu	30.2 (95% CI) 29.1–31.3)
<b>2g</b>	6-Cl	3-Cl		<i>tert</i> -Bu	34.2 (95% CI) 30.7–38.0)
<b>2h</b>	6-Cl	3-Cl	CO <sub>2</sub> CH <sub>2</sub> CH <sub>3</sub>	Cyclohexyl	25.5 (95% CI) 24.7–26.4)
<b>2i</b>	6-Cl	3-Cl	CO <sub>2</sub> CH <sub>2</sub> CH <sub>3</sub>	<i>tert</i> -Bu	N.D.
<b>2j</b>	6-Cl	4-Cl	CO <sub>2</sub> CH <sub>2</sub> CH <sub>3</sub>	Cyclohexyl	39.1 (95% CI) 37.4–40.8)
<b>2k</b>	6-Cl	4-Cl	CO <sub>2</sub> CH <sub>2</sub> CH <sub>3</sub>	<i>tert</i> -Bu	30.2 (95% CI) 27.2–33.6)
<b>2l</b>	6-Cl	3-F	CO <sub>2</sub> CH <sub>2</sub> CH <sub>3</sub>	Cyclohexyl	27.5 (95% CI) 25.8–29.3)
<b>2m</b>	6-Cl	3-F	CO <sub>2</sub> CH <sub>2</sub> CH <sub>3</sub>	<i>tert</i> -Bu	44.8 (95% CI) 40.7–49.3)
<b>2n</b>	6-Cl	3-F	CO <sub>2</sub> CH <sub>2</sub> CH <sub>3</sub>	Ph	29.9 (95% CI) 28.7–31.2)
<b>2o</b>	6-Cl	4-F	CO <sub>2</sub> CH <sub>2</sub> CH <sub>3</sub>	Cyclohexyl	31.7 (95% CI) 30.0–33.5)
<b>2p</b>	6-Cl	4-F	CO <sub>2</sub> CH <sub>2</sub> CH <sub>3</sub>	<i>tert</i> -Bu	49.9 (95% CI) 47.9–51.9)
<b>2q</b>	6-Cl	3-Cl	CO <sub>2</sub> CH <sub>2</sub> CH <sub>3</sub>	4-Cl-Ph	18.0 (95% CI) 17.6–18.5)
<b>2r</b>	6-Cl	3-Cl	CO <sub>2</sub> CH <sub>2</sub> CH <sub>3</sub>	<i>tert</i> -Bu	35.1 (95% CI) 33.1–37.3)

(continued on next page)

Table 2 (continued)

Compound	R <sup>1</sup>	R <sup>2</sup>	R <sup>3</sup>	R <sup>4</sup>	IC <sub>50</sub> (μM) HCT116
2s	6-Cl-5-F	3-F-Ph	CO <sub>2</sub> CH <sub>2</sub> CH <sub>3</sub>	<i>tert</i> -Bu	41.9 (95% CI 39.1–44.9)
3a	6-Cl	3-OH-Ph	CO <sub>2</sub> CH <sub>2</sub> CH <sub>3</sub>	4-Cl-Ph	33.7 (95% CI 32.4–35.0)
3b	6-Cl	3-OH-Ph		4-Cl-Ph	18.8 (95% CI 17.6–20.0)
3c	6-Cl	3-OH-Ph		4-Cl-Ph	27.2 (95% CI 26.3–28.0)
3d	6-Cl	3-OH-Ph		4-Cl-Ph	27.0 (95% CI 26.1–28.0)
3e	6-Cl	3-OH-Ph		4-Cl-Ph	37.2 (95% CI 36.2–38.1)
3f	6-Cl	3-OH-Ph		4-Cl-Ph	20.9 (95% CI 19.4–22.5)
3g	6-Cl	3-OH-Ph		4-Cl-Ph	>50
3h	6-Cl	3-OH-Ph		4-Cl-Ph	N.D.

Each value is a mean (IC<sub>50</sub>, 95% CI) of three independent experiments.  
N.D. – not determined (no dose-response observed).

cells treated with compounds **2q** and **3b**, to evaluate if the loss of cell viability was associated with cell death. The LDH assay indirectly indicates if the integrity of the plasma membrane in SJSA-1 cells is compromised after being exposed to derivatives **2q** or **3b**. At 10 μM (IC<sub>50</sub> concentration) for 96 h, the amount of LDH detected was similar to the one observed for the vehicle-treated cells (DMSO). At 15 μM (1.5 times IC<sub>50</sub> concentration) of derivative **3b** and for the same period of incubation time, SJSA-1 cells showed approximately 1.3-fold increase in LDH release (Fig. 8A), while for compound **2q**, a 1.3-fold and a 1.6-fold increase in LDH release was observed at 15 μM (IC<sub>50</sub> concentration) and 22.5 μM (1.5 times IC<sub>50</sub> concentration), respectively.

Cell death via apoptosis was investigated by flow cytometry, after Annexin V-FITC/7-AAD double-staining of SJSA-1 cells (Fig. 9). This assay allows determining the percentage of viable cells (FITC<sup>-</sup>/7-AAD<sup>-</sup>) as well as early (FITC<sup>+</sup>/7-AAD<sup>-</sup>) and late apoptotic (FITC<sup>+</sup>/7-AAD<sup>+</sup>) cells. Most SJSA-1 cells exposed to DMSO (control) are viable (between 94.3 and 99.2%), which indicates that the plasma membrane is not damaged. In cells exposed to 15 μM of derivative **2q**, there is almost no decrease of viable cells (98.57% versus DMSO 99.2%), but treatment with a higher dose (22.5 μM) leads to a decrease of viable SJSA-1 cells (92.7%) and a consequent increase of early (2.9% versus 0.3%) and late (4.3% versus 0.6%) apoptotic cells (Fig. 9A). In cells exposed to 10 μM of derivative **3b**, there is a slight decrease of viable cells to 90.5% versus DMSO 94.3%, representing a consequent increase of early (4.1% versus 1.9%) and late (5.2% versus 3.7%) apoptotic cells. At 15 μM, the

percentage of viable SJSA-1 cells reached 65.3% and a similar percentage of early (14.4%) and late (19.1%) apoptotic cells was observed (Fig. 9B). Furthermore, microscopic visualization of SJSA-1 cells treated with vehicle control or derivatives **2q** and **3b** for 96 h, showed significant morphological differences. While for compound **2q**, at the IC<sub>50</sub> concentration, no significant morphological differences were observed, at 1.5 times IC<sub>50</sub> concentration, there was a substantial decrease of cell growth versus the control (Fig. 9C). For compound **3b**, at the IC<sub>50</sub> concentration, there was a substantial decrease of cell growth versus control, but with 1.5 times IC<sub>50</sub> concentration of **3b**, the SJSA-1 cells exhibited loss of volume, an indication of cell death (Fig. 9C).

Representative plots are shown. Values representative of mean ± SD of three independent experiments. Ordinary one-way ANOVA or Kruskal-Wallis test followed by Bonferroni's or Dunn's multiple comparisons test, respectively. \**p* < 0.05; \*\**p* < 0.01; <sup>δ</sup>*p* < 0.0001 vs. DMSO. Compounds **2q** and **3b** induce cell cycle arrest in SJSA-1 cells. To go deeper into the mechanisms induced by compounds **2q** and **3b**, cell cycle progression was also evaluated to better understand the loss of cell viability. SJSA-1 cells were exposed for 96 h to derivatives **2q** (15 μM and 22.5 μM) and **3b** (10 μM and 15 μM). After the incubation time, cells were collected and stained with propidium iodide (PI), the most used dye for cellular DNA content, that allows the quantification of cell cycle distribution by flow cytometry. Fig. 10 shows the percentage of cells in each phase (G0/G1, S, or G2/M). Spiropyrazoline oxindoles **2q** and **3b** induced a significant accumulation of cells in G0/G1 phase while decreased the percentage of cells in both S and G2/M phases, compared to control (DMSO). In addition, the increase of cells in G0/G1 phase occurs in a concentration-dependent manner of **2q** (15 μM-67.5% versus 22.5 μM-82.2%) and **3b** (10 μM-74.9% versus 15 μM-91.8%). Collectively, these results indicate that the loss of viability is due to cell cycle arrest and partially via cell apoptosis induction.

**Biochemical activity of candidate compounds against MDM2-p53 and MDM4-p53 interactions.** The ability of compounds **2a**, **2q**, **3b-c** and **3f** to block the p53 interactions with MDM2 and MDM4 was demonstrated by immunoenzymatic assays (Table 4). From this set of compounds, only derivative **3c** didn't inhibit both PPIs. Compound **3b** was selective for MDM2-p53 PPI over MDM4-p53 PPI, while compounds **2a** and **2q** showed IC<sub>50</sub> values in the low nM range for both MDM2-p53 and MDM4-p53 PPIs.

To understand why compound **3b** was less active for MDM4-p53 PPI, a molecular mechanics/Poisson-Boltzmann surface area (MM-PBSA) study was performed on the complex between the compound and MDM2 and MDM4 (results in SI). To test the effect of R<sup>3</sup> substituent in **3b**, the spiropyrazoline oxindole **3a** containing an ester group at R<sup>3</sup> and HRN (molecule co-crystallized in the crystallographic structure coded by PDB-ID 6Q9S) were used for comparison. The calculations were done with a slight modification in the solvent-exposed acidic moiety of HRN that was changed to a neutral OH (HRN\_OH), to get all molecules in a neutral state for an electrostatic contribution in the same range.

The major differences between the **3a**, **3b**, and HRN\_OH are found in the van der Waals energy contribution that has higher complex stabilization capability in **3b**, closing the gap to HRN\_OH, although **3b** has higher penalty in the polar solvation energy.

It is important to stress that although all molecular dynamics runs started from the initial molecular docking predictions, the binding poses were stable for HRN\_OH and **3a** while a rotation occurs for **3b**. In **3b**, the R<sup>4</sup> (4-Cl-Ph) initially located in the Phe19 pocket moves into the Trp23 pocket, previously occupied by the indole, while this one moves to the Leu26 position (Fig. 11). This rotation allows R<sup>3</sup> of **3b** to have closer contact with MDM4 while making hydrogen bonds with MDM4<sup>Tyr67</sup> through the amide carbonyl and the amide hydrogen and another one with MDM4<sup>Val93</sup> through the 3-OH-Ph of R<sup>2</sup>.

A similar study with **3b** performed on the MDM2 structure also reproduced the higher experimental activity of **3b** on MDM2, showing that all energy contributions, but polar solvation energy, are more favorable in the MDM2 complex, although it is the van der Waals energy

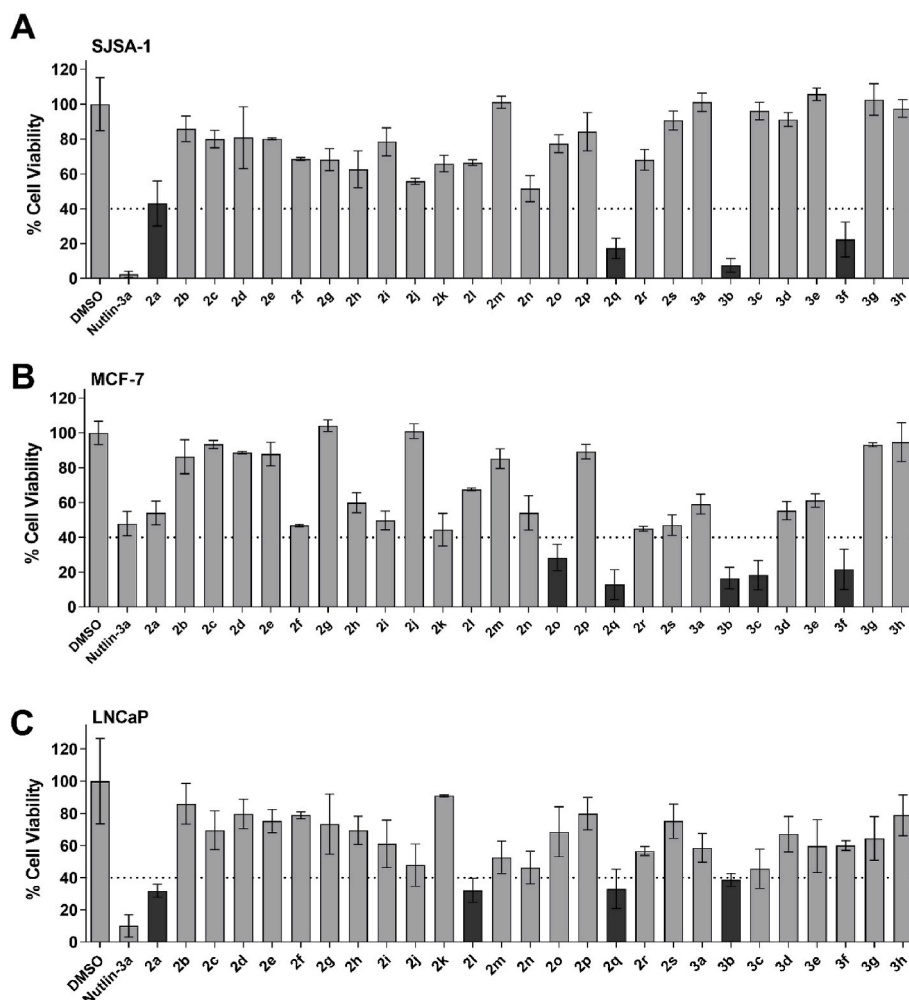


**Fig. 6.** - *In vitro* antiproliferative effect of spiropyrazoline oxindoles **2a-s** and **3a-h** determined by the MTS assay in: A) SJSA-1 cells (20  $\mu$ M); B) MCF-7 cells (20  $\mu$ M); C) LNCaP cells (10  $\mu$ M). Nutlin-3a was used as positive control and DMSO (vehicle) as negative control. Each value is a mean  $\pm$  SD of three independent experiments. A 40% cellular viability threshold was established, and compounds with higher antiproliferative activity are represented by darker bars.

that contributes the most. Moreover, it also confirmed that the pose containing the indole inside the Trp23 pocket is, once again, not always the one producing the most stable complex.

### 3. Conclusions

In this work, the spiropyrazoline oxindole scaffold was virtually optimized by molecular docking to target the main p53 negative regulators, MDM2 and MDM4, to obtain novel small molecule dual MDM2/4 inhibitors. Based on the structural requirements identified, twenty-seven spiropyrazoline oxindoles were prepared and their antiproliferative activity evaluated in four cancer cell lines that overexpress MDM2 and/or MDM4. Compounds **2q** and **3b** were the most promising derivatives with  $IC_{50}$  values ranging from 9.7 to 15.6  $\mu$ M in SJSA-1, LNCaP, and MCF-7 cell lines, and non-toxic in HEK293T cells. Further assays indicated that compounds **2q** and **3b** control cell growth by targeting G0/G1 cell cycle checkpoint and induce apoptosis in SJSA-1 cells, both in a concentration-dependent manner. Moreover, three of the best compounds showed nanomolar activity blocking both MDM2-p53 and MDM4-p53 PPIs, while one compound blocked more selectively the MDM2-p53 PPI. Collectively, the presented results show the potential of spiropyrazoline oxindoles as anticancer agents by dual inhibition of MDM2/4-p53 PPIs.

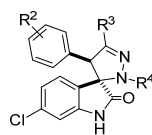
## 4. Experimental section

### 4.1. Chemical synthesis

Chemicals were purchased from commercial suppliers and used without further purification. Triethylamine was dried over potassium hydroxide, distilled, and stored with molecular sieves (4  $\text{\AA}$ ), which were previously activated by heat *in vacuo*. Reaction solvents were used as supplied (analytical or HPLC grade) without purification. All the primary amines and anilines were purchased with exception of the aniline used to prepare derivative **3b** (synthetic procedures in SI). Thin-layer chromatography (TLC) was carried out on normal phase Merck silica gel 60 F<sub>254</sub> aluminum sheets and visualized by UV light ( $\lambda_{\text{max}} = 254/360$  nm). TLC plates were dipped in ninhydrin or potassium permanganate solutions if necessary. Flash column chromatography was performed on normal phase Merck Silica Gel (200–400 mesh ASTM).  $^1\text{H}$  NMR and  $^{13}\text{C}$  NMR spectra were recorded on Bruker 300 Ultra-Shield (300 MHz) spectrometer.  $^1\text{H}$  and  $^{13}\text{C}$  NMR chemical shifts are given as  $\delta_{\text{H}}$  and  $\delta_{\text{C}}$ , respectively, in parts per million (ppm), relative to tetramethylsilane (TMS) where  $\delta$  (TMS) = 0.00 ppm. The spectra were referenced to the solvent peak and coupling constants ( $J$ ) are quoted in hertz (Hz). Spectra were assigned using the following 2D NMR experiments: COSY, APT, HSQC, and HMBC. Multiplicities in  $^1\text{H}$  NMR spectra are indicated by s (singlet), d (doublet), dd (doublet of doublets), dt (doublet of triplets), t (triplet), tdd (triplet of doublets of doublets), m (multiplet) or br s (broad

Table 3

– *In vitro* antiproliferative activities (IC<sub>50</sub>) of the most promising spiropyrazoline oxindoles in SJSA-1, LNCaP, and MCF-7 cells.



Compound	IC <sub>50</sub> (μM) SJSA-1	IC <sub>50</sub> (μM) LNCaP	IC <sub>50</sub> (μM) MCF-7
2a	20.8 (95% CI 19.8–21.8)	12.6 (95% CI 11.3–14.2)	N.D.
2l	N.D.	13.1 (95% CI 10.9–15.7)	N.D.
2o	N.D.	N.D.	20.2 (95% CI 18.6–22.0)
2q	15.6 (95% CI 14.3–16.9)	10.7 (95% CI 9.8–11.7)	15.6 (95% CI 14.7–16.5)
3b	10.7 (95% CI 10.3–11.1)	11.4 (95% CI 9.9–13.1)	9.7 (95% CI 9.4–10.1)
3c	N.D.	N.D.	14.3 (95% CI 13.2–15.4)
3f	17.4 (95% CI 16.3–18.5)	11.5 (95% CI 10.6–12.4)	12.4 (95% CI 12.0–12.8)

Each value is a mean (IC<sub>50</sub>, 95% CI) of three independent experiments. N.D. – not determined (no dose-response observed).

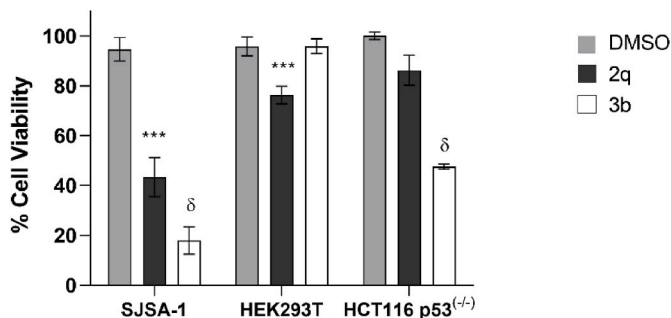


Fig. 7. - Effect of derivatives **2q** and **3b** in SJSA-1 cells (15 μM), non-tumoral HEK293T cells (15 μM), and HCT116 p53<sup>(-/-)</sup> cells (20 μM). Percentage of cell viability determined by MTS assay after 96 h (SJSA-1 and HEK293T) or 48 h (HCT116 p53<sup>(-/-)</sup>) of compounds' incubation. Each value is a mean ± SD of three independent experiments. Ordinary one-way ANOVA followed by Bonferroni's multiple comparisons test. \*\*\**p* < 0.001; <sup>δ</sup>*p* < 0.0001 vs. respective cell line DMSO control.

singlet). Multiplicity in <sup>13</sup>C NMR spectra can be given as d (doublet), in the case of compounds with C–F bonds. Melting points were determined using a Kofler camera Bock monoscope M. Low-resolution mass spectra (LRMS) were recorded on a Micromass® Quattro Micro triple quadrupole spectrometer (ESI) (Waters®, Ireland). In MS experiments, solutions were prepared in MeOH or MeCN, and *m/z* values are reported in Daltons. The purity of final compounds was assessed by LaChrom HPLC constituted by a Merck Hitachi pump L-7100, Merck Hitachi autosampler L-7250 and a Merck Hitachi UV detector L-7400 set at 250 nm. A LiChrospher® 100C8 [5 μm, 100 Å, 250 mm × 4.0 mm] reverse phase column was used with a constant flow rate of 1.0 mL min<sup>-1</sup> and (A) gradient method of 13 min from 95:5H<sub>2</sub>O:MeCN to 5:95H<sub>2</sub>O:MeCN; (B) isocratic method of 13 min using 80:20 MeCN:H<sub>2</sub>O (0.1% formic acid); (C) isocratic method of 13 min using 60:40 MeCN:H<sub>2</sub>O (0.1% formic acid); (D) gradient method of 16 min from 50:50H<sub>2</sub>O:MeOH to 10:90H<sub>2</sub>O:MeOH.

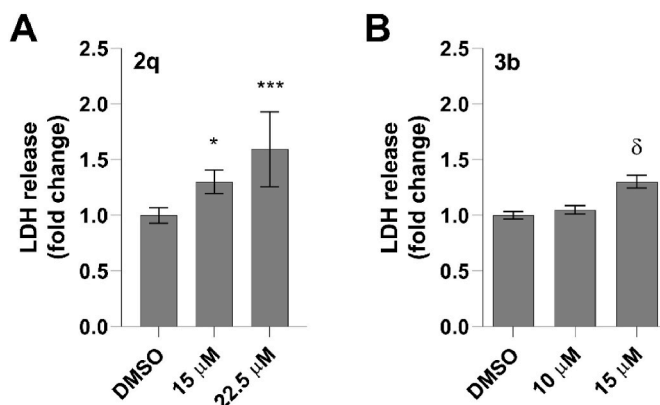


Fig. 8. - Effect of spiropyrazoline oxindoles **2q** and **3b** in LDH release in SJSA-1 cells after 96 h incubation. Cells were treated with vehicle control (DMSO), IC<sub>50</sub> or 1.5 times IC<sub>50</sub> concentration of A) **2q**, 15 and 22.5 μM, respectively, or B) **3b**, 10 and 15 μM, respectively. Each value is a mean ± SD of three independent experiments. Ordinary one-way ANOVA followed by Bonferroni's multiple comparisons test. \**p* < 0.05; \*\*\**p* < 0.001; <sup>δ</sup>*p* < 0.0001 vs. DMSO.

#### 4.1.1. General procedure for the synthesis of spiropyrazoline oxindoles (**2a**, **2c**, **2 h-s** and **3a**)

3-Methylene indolin-2-one (1.0 eq.) and hydrazonyl chloride (1.5 eq.) were added to a pressure tube, under nitrogen atmosphere. MeCN (0.18 mmol/mL) was added at room temperature, followed by Et<sub>3</sub>N (3.0 eq.). The reaction mixture was stirred at 90 °C for 15 h and then concentrated *in vacuo*. The crude residue was purified by silica gel flash chromatography to yield the desired spiropyrazoline oxindole.

**Ethyl 6-chloro-4'-(3-chloro-2-fluorophenyl)-2'-cyclohexyl-2-oxo-2',4'-dihydrospiro [indoline-3,3'-pyrazole]-5'-carboxylate (2a):** 6-Chloro-3-(3-chloro-2-fluorobenzylidene)indolin-2-one (**4a**) (50 mg, 0.162 mmol, 1.0 eq.) and ethyl 2-chloro-2-(2-cyclohexylhydrazono)acetate (**5a**) (57 mg, 0.243 mmol, 1.5 eq.) were added to a pressure tube, under nitrogen atmosphere. MeCN (1 mL) was added at room temperature, followed by Et<sub>3</sub>N (68 μL, 0.487 mmol, 3.0 eq.). The reaction mixture was stirred at 90 °C for 15 h and then concentrated *in vacuo*. The crude residue was purified by silica gel flash chromatography (elution with CH<sub>2</sub>Cl<sub>2</sub> to 2% MeOH in CH<sub>2</sub>Cl<sub>2</sub>) to yield the title compound (73 mg, 0.145 mmol, 89%). The compound was recrystallized in Et<sub>2</sub>O/*n*-heptane resulting in a pale-yellow solid; R<sub>f</sub> 0.65 (5% MeOH in CH<sub>2</sub>Cl<sub>2</sub>); m.p.: 132–135 °C; <sup>1</sup>H NMR (300 MHz, CDCl<sub>3</sub>) δ<sub>H</sub> 8.67 (s, 1H, NH), 7.23 (t, *J* = 7.83 Hz, 1H, ArH), 7.10–6.90 (m, 3H, ArH), 6.66 (d, *J* = 8.1 Hz, 1H, ArH), 6.17 (d, *J* = 5.58 Hz, 1H, ArH), 5.14 (s, 1H, CH), 4.28–4.16 (m, 2H, CH<sub>2</sub>CH<sub>3</sub>), 2.80–2.65 (m, 1H, CH-cyclohexyl), 1.98–1.86 (m, 1H, CH<sub>2</sub>), 1.75–1.40 (m, 7H, CH<sub>2</sub>), 1.19 (t, *J* = 7.17 Hz, 3H, CH<sub>2</sub>CH<sub>3</sub>), 1.07–0.92 (m, 2H, CH<sub>2</sub>); <sup>13</sup>C NMR (75 MHz; CDCl<sub>3</sub>) δ<sub>C</sub> 177.5 (C=O), 161.6 (C=OCH<sub>2</sub>CH<sub>3</sub>), 155.8 (d, *J*<sub>C-F</sub> = 249.53 Hz, C–F), 142.2 (Cq), 136.0 (Cq), 133.7 (C=N), 130.1 (ArCH), 127.2 (ArCH), 126.8 (ArCH), 124.5 (d, *J* = 14.99 Hz, Cq), 124.3 (d, *J* = 4.55 Hz, ArCH), 122.5 (Cq), 122.3 (ArCH), 121.3 (d, *J* = 18.02 Hz, Cq), 111.3 (ArCH), 77.2 (Cq-spiro), 60.8 (CH<sub>2</sub>CH<sub>3</sub>), 59.2 (CH-cyclohexyl), 51.7 (CH), 33.1 (CH<sub>2</sub>), 32.4 (CH<sub>2</sub>), 25.5 (CH<sub>2</sub>), 25.0 (CH<sub>2</sub>), 14.2 (CH<sub>2</sub>CH<sub>3</sub>); LRMS *m/z* (ESI<sup>+</sup>) [Found: 504, C<sub>25</sub>H<sub>24</sub>Cl<sub>2</sub>FN<sub>3</sub>O<sub>3</sub> requires [M+H]<sup>+</sup> 504; HPLC Method 1 (A): Retention time 10.4 min, 98.8%.

**Ethyl 2'-(*tert*-butyl)-6-chloro-4'-(3-chloro-2-fluorophenyl)-2-oxo-2',4'-dihydrospiro [indoline-3,3'-pyrazole]-5'-carboxylate (2c):** 6-Chloro-3-(3-chloro-2-fluorobenzylidene)indolin-2-one (**4a**) (50 mg, 0.162 mmol, 1.0 eq.) and ethyl 2-(2-(*tert*-butyl)hydrazono)-2-chloroacetate (**5b**) (50 mg, 0.243 mmol, 1.5 eq.) were added to a pressure tube, under nitrogen atmosphere. MeCN (1 mL) was added at room temperature, followed by Et<sub>3</sub>N (68 μL, 0.487 mmol, 3.0 eq.). The reaction mixture was stirred at 90 °C for 15 h and then concentrated *in vacuo*. The crude residue was purified by silica gel flash chromatography (elution with CH<sub>2</sub>Cl<sub>2</sub> to 2% MeOH in CH<sub>2</sub>Cl<sub>2</sub>) to yield the title compound



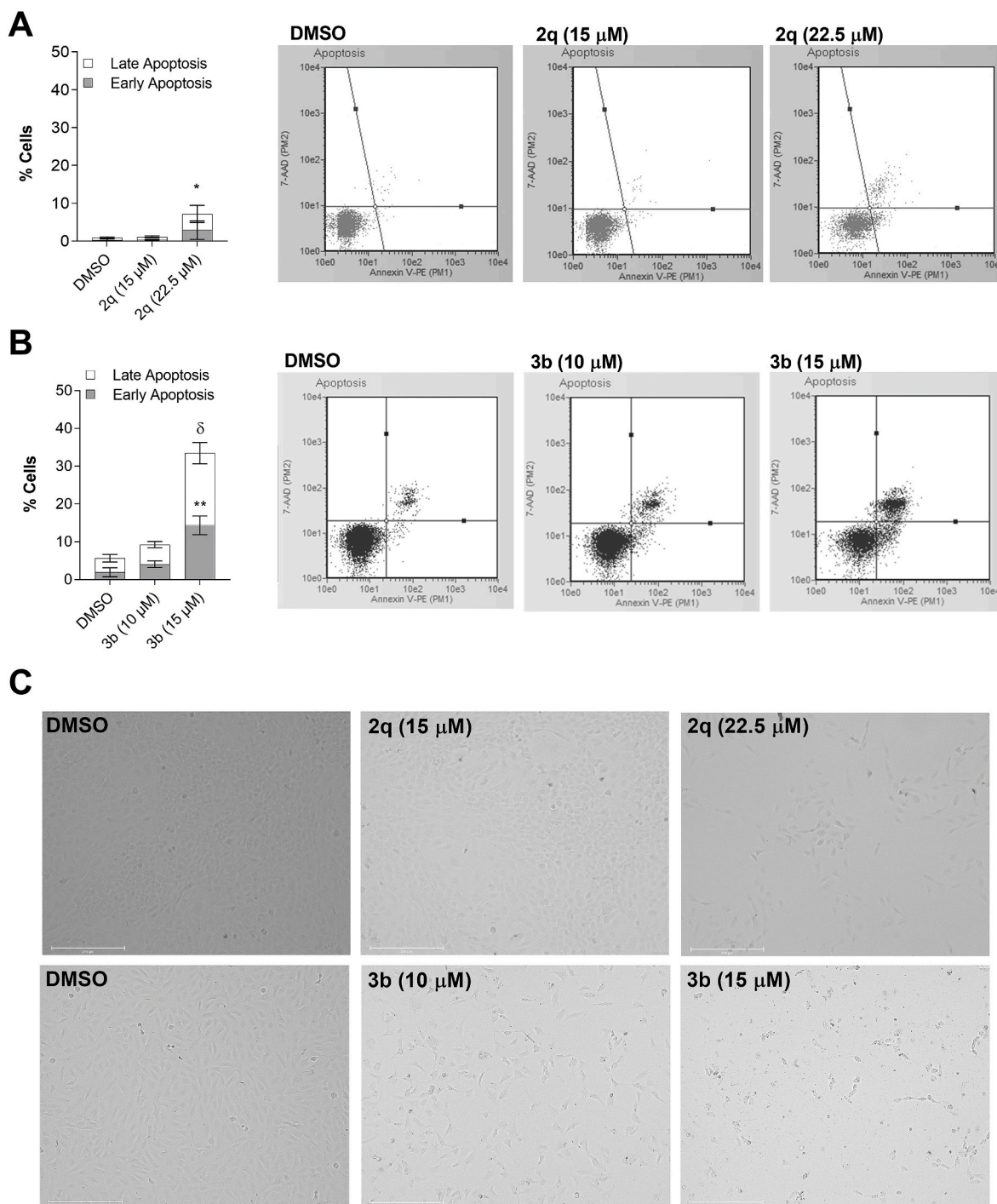


**Fig. 9.** – Evaluation of apoptosis as cell death mechanism. SJS-1 cells were incubated with vehicle control (DMSO) or spiropyrazoline oxindoles **2q** and **3b** for 96 h. Annexin V-FITC/7-AAD double-staining procedure (flow cytometry) was used to evaluate apoptosis in SJS-1 cells incubated with: A) 15 μM and 22.5 μM of **2q**; or B) 10 μM and 15 μM of **3b**. C) Brightfield microscopy images representative of SJS-1 cell morphology after incubation with DMSO, **2q** or **3b** for 96 h. Scale bar, 275 μm.

(70 mg, 0.146 mmol, 90%). The compound was recrystallized in Et<sub>2</sub>O/*n*-heptane resulting in a white solid; R<sub>f</sub> 0.56 (5% MeOH in CH<sub>2</sub>Cl<sub>2</sub>); m.p.: 178–179 °C; <sup>1</sup>H NMR (300 MHz, CDCl<sub>3</sub>) δ<sub>H</sub> 8.77 (s, 1H, NH), 7.19 (t, *J* = 6.4 Hz, 1H, ArH), 7.08–6.71 (m, 3H, ArH), 6.64 (d, *J* = 8.1 Hz, 1H, ArH), 6.35 (d, *J* = 7.77 Hz, 1H, ArH), 5.22 (s, 1H, CH), 4.28–4.10 (m, 2H, CH<sub>2</sub>CH<sub>3</sub>), 1.25 (s, 9H, C(CH<sub>3</sub>)<sub>3</sub>), 1.16 (t, *J* = 7.0 Hz, 3H, CH<sub>2</sub>CH<sub>3</sub>); <sup>13</sup>C NMR (75 MHz; CDCl<sub>3</sub>) δ<sub>C</sub> 178.5 (C=O), 161.6 (C=OCH<sub>2</sub>CH<sub>3</sub>), 155.9 (d, *J*<sub>C-F</sub> = 245.11 Hz, C-F), 141.1 (Cq), 135.6 (C=N), 132.4 (Cq), 130.0 (ArCH), 127.6 (ArCH), 127.1 (ArCH), 124.9 (Cq), 124.5 (d, *J* = 15.18

Hz, Cq), 124.1 (d, *J* = 4.28 Hz, ArCH), 122.0 (ArCH), 121.1 (d, *J* = 19.34 Hz, Cq), 111.3 (ArCH), 77.2 (Cq-spiro), 60.8 (C(CH<sub>3</sub>)<sub>3</sub>), 60.7 (CH<sub>2</sub>CH<sub>3</sub>), 54.2 (CH), 29.5 (C(CH<sub>3</sub>)<sub>3</sub>), 14.1 (CH<sub>2</sub>CH<sub>3</sub>); LRMS m/z (ESI<sup>+</sup>) [Found: 478, C<sub>23</sub>H<sub>22</sub>Cl<sub>2</sub>FN<sub>3</sub>O<sub>3</sub> requires [M+H]<sup>+</sup> 478; HPLC Method 1 (A): Retention time 9.4 min, 100%.

**Ethyl 6-chloro-4'-(3-chlorophenyl)-2'-cyclohexyl-2-oxo-2',4'-dihydrospiro[indoline-3,3'-pyrazole]-5'-carboxylate (2h):** 6-Chloro-3-(3-chlorobenzylidene)indolin-2-one (**4b**) (100 mg, 0.345 mmol, 1.0 eq.) and ethyl 2-chloro-2-(2-cyclohexylhydrazono)acetate

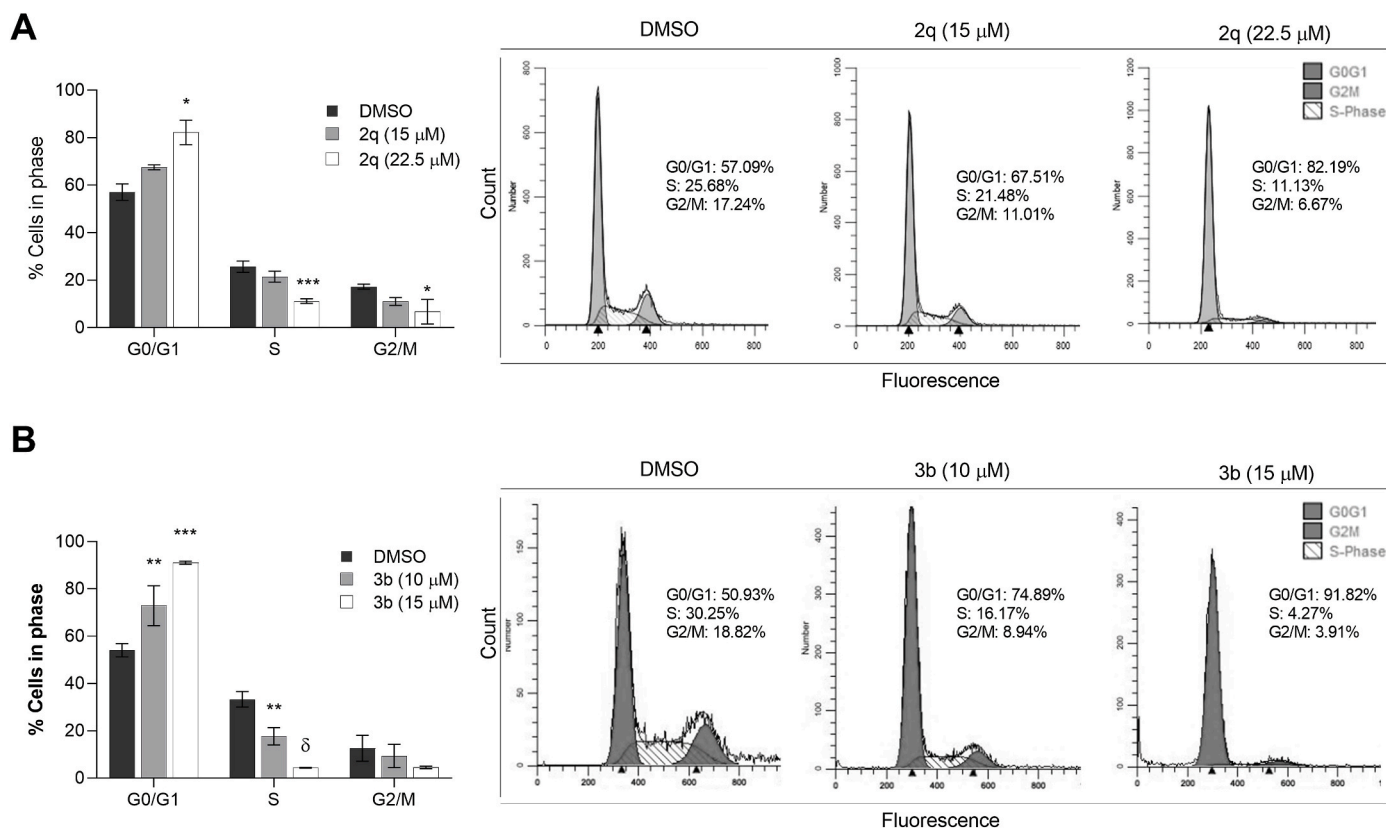


**Fig. 10.** - Effect of spiroprazolone oxindoles **2q** and **3b** on SJS-1 cell cycle progression. Cells were exposed for 96 h to vehicle control DMSO or to: A) **2q** (15 μM and 22.5 μM); or B) **3b** (10 μM and 15 μM). PI was used to stain cellular DNA content, measured by flow cytometry. The cell cycle distribution of SJS-1 cells was determined using Mod Fit LT 4.1 software. The histograms represent one of three independent experiments. The graph bar is a mean ± SD of three independent experiments. Ordinary one-way ANOVA or Kruskal-Wallis followed by Bonferroni's or Dunn's multiple comparisons tests, respectively. \* $p < 0.05$ ; \*\* $p < 0.01$ ; \*\*\* $p < 0.001$ ; <sup>δ</sup> $p < 0.0001$  vs. DMSO.

**Table 4**

- IC<sub>50</sub> values obtained in the dissociation of p53-MDMs complexes by compounds **1**, **2a**, **2q**, **3b**, **3c** and **3f** using immunoenzymatic assays.

Compound	IC <sub>50</sub> (nM) MDM2-p53	IC <sub>50</sub> (nM) MDM4-p53
<b>2a</b>	18.5 ± 2.1	14.8 ± 5.2
<b>2q</b>	70.7 ± 5.1	81.4 ± 4.0
<b>3b</b>	26.1 ± 3.6	219.0 ± 9.0
<b>3c</b>	N. A. <sup>a</sup>	N. A.
<b>3f</b>	35.9 ± 5.0	57.4 ± 2.9
<b>1</b>	144.0 ± 13.0	295.0 ± 24.0

<sup>a</sup> N.A. - not active for the tested concentrations.

(**5a**) (120 mg, 0.517 mmol, 1.5 eq.) were added to a pressure tube, under nitrogen atmosphere. MeCN (2.0 mL) was added at room temperature, followed by Et<sub>3</sub>N (144 μL, 1.03 mmol, 3.0 eq.). The reaction mixture was stirred at 90 °C for 15 h and then concentrated *in vacuo*. The crude residue was purified by silica gel flash chromatography (elution with CH<sub>2</sub>Cl<sub>2</sub>) to yield the title compound (121 mg, 0.248 mmol, 72%). The compound was recrystallized in Et<sub>2</sub>O/*n*-heptane resulting in a white solid; R<sub>f</sub> 0.56 (5% MeOH in CH<sub>2</sub>Cl<sub>2</sub>); m.p.: 175–176 °C; <sup>1</sup>H NMR (300 MHz, CDCl<sub>3</sub>) δ<sub>H</sub> 8.78 (s, 1H, NH), 7.22–7.08 (m, 2H, ArH), 6.92–6.86 (m, 2H, ArH), 6.79 (d, *J* = 7.0 Hz, 1H, ArH), 6.68 (dd, *J* = 8.1, 1.9 Hz, 1H, ArH), 6.30 (d, *J* = 8.1 Hz, 1H, ArH), 4.77 (s, 1H, CH), 4.32–4.11 (m, 2H, CH<sub>2</sub>CH<sub>3</sub>), 2.87–2.53 (m, 1H, CH<sub>2</sub>), 2.04–1.90 (m, 1H, CH<sub>2</sub>), 1.81–1.58 (m, 6H, CH<sub>2</sub>), 1.56–1.49 (m, 1H, CH<sub>2</sub>), 1.18 (t, *J* = 7.1 Hz, 3H, CH<sub>2</sub>CH<sub>3</sub>), 1.14–0.99 (m, 2H, CH<sub>2</sub>); <sup>13</sup>C NMR (75 MHz; CDCl<sub>3</sub>) δ<sub>C</sub> 178.1 (C=O), 161.7 (C=OCH<sub>2</sub>CH<sub>3</sub>), 141.7 (Cq), 136.8 (Cq), 135.9 (Cq), 135.8 (C=N), 134.4 (Cq), 129.8 (ArCH), 128.3 (ArCH), 128.1 (ArCH), 127.3 (ArCH), 126.6 (ArCH), 122.5 (ArCH), 122.3 (Cq), 111.2 (ArCH), 78.3

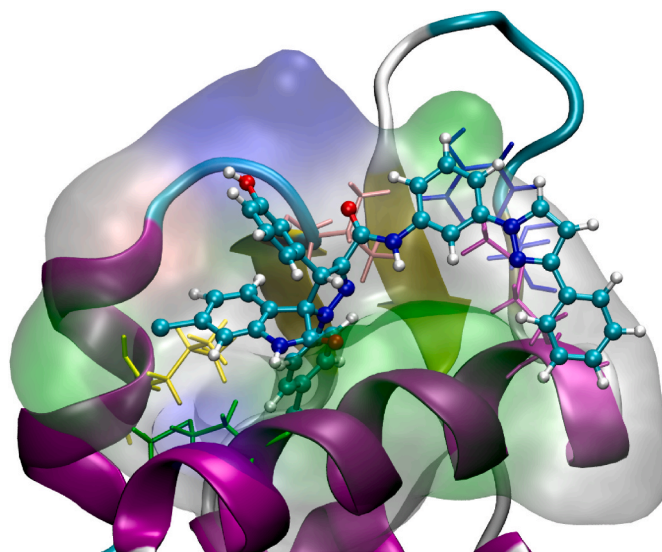


**Fig. 11.** - Conformation of compound **3b** (CPK) at the end of the MD production run showing the clockwise rotation for a better fitting in the MDM4 binding pocket. In licorice and green MDM<sup>4</sup>Met54, MDM<sup>4</sup>Tyr67 in blue, MDM<sup>4</sup>Met62 in purple, MDM<sup>4</sup>Val93 in pink, and MDM<sup>4</sup>Leu99 in yellow.

(Cq-spiro), 60.9 (CH<sub>2</sub>CH<sub>3</sub>), 59.1 (CH-cyclohexyl), 58.8 (CH), 33.0 (CH<sub>2</sub>), 32.3 (CH<sub>2</sub>), 25.4 (CH<sub>2</sub>), 25.0 (CH<sub>2</sub>), 14.1 (CH<sub>2</sub>CH<sub>3</sub>); LRMS m/z (ESI<sup>+</sup>) [Found: 486, C<sub>25</sub>H<sub>25</sub>Cl<sub>2</sub>N<sub>3</sub>O<sub>3</sub> requires [M+H]<sup>+</sup> 486]; HPLC Method 1 (A): Retention time 10.5 min, 99.6%.

**Ethyl 2'-(tert-butyl)-6-chloro-4'-(3-chlorophenyl)-2-oxo-2',4'-dihydrospiro [indoline-3,3'-pyrazole] -5'-carboxylate (2i):** 6-Chloro-3-(3-chlorobenzylidene)indolin-2-one (**4b**) (202 mg, 0.696 mmol, 1.0 eq.) and ethyl 2-(2-(tert-butyl)hydrazono)-2-chloroacetate (**5b**) (216 mg, 1.04 mmol, 1.5 eq.) were added to a pressure tube, under nitrogen atmosphere. MeCN (3.8 mL) was added at room temperature, followed by Et<sub>3</sub>N (291  $\mu$ L, 2.09 mmol, 3.0 eq.). The reaction mixture was stirred at 90 °C for 15 h and then concentrated *in vacuo*. The crude residue was purified by silica gel flash chromatography (elution with CH<sub>2</sub>Cl<sub>2</sub>) to yield the title compound (258 mg, 0.561 mmol, 81%). The compound was recrystallized in Et<sub>2</sub>O/*n*-heptane resulting in a white solid; R<sub>f</sub> 0.52 (5% MeOH in CH<sub>2</sub>Cl<sub>2</sub>); m.p.: 221–224 °C; <sup>1</sup>H NMR (300 MHz, CDCl<sub>3</sub>)  $\delta$ <sub>H</sub> 8.71 (s, 1H, NH), 7.13–7.01 (m, 2H, ArH), 6.87 (t, *J* = 1.8 Hz, 1H, ArH), 6.79 (d, *J* = 1.8 Hz, 1H, ArH), 6.76 (dt, *J* = 7.1, 1.6 Hz, 1H, ArH), 6.69 (dd, *J* = 8.1, 1.9 Hz, 1H, ArH), 6.55 (d, *J* = 8.1 Hz, 1H, ArH), 4.87 (s, 1H, CH), 4.32–4.02 (m, 2H, CH<sub>2</sub>CH<sub>3</sub>), 1.25 (s, 9H, C(CH<sub>3</sub>)<sub>3</sub>), 1.15 (t, *J* = 7.1 Hz, 3H, CH<sub>2</sub>CH<sub>3</sub>); <sup>13</sup>C NMR (75 MHz; CDCl<sub>3</sub>)  $\delta$ <sub>C</sub> 178.9 (C=O), 161.8 (C=OOCH<sub>2</sub>CH<sub>3</sub>), 140.3 (Cq), 136.7 (Cq), 135.4 (C=N), 134.2 (Cq), 134.0 (Cq), 129.5 (ArCH), 128.4 (ArCH), 127.9 (ArCH), 127.7 (ArCH), 126.6 (ArCH), 125.0 (Cq), 122.1 (ArCH), 111.1 (ArCH), 78.3 (Cq-spiro), 61.6 (CH), 60.7 (CH<sub>2</sub>CH<sub>3</sub>), 60.5 (C(CH<sub>3</sub>)<sub>3</sub>), 29.6 (C(CH<sub>3</sub>)<sub>3</sub>), 14.1 (CH<sub>2</sub>CH<sub>3</sub>); LRMS m/z (ESI<sup>+</sup>) [Found: 460, C<sub>23</sub>H<sub>23</sub>Cl<sub>2</sub>N<sub>3</sub>O<sub>3</sub> requires [M+H]<sup>+</sup> 460]; HPLC Method 1 (A): Retention time 9.5 min, 99.4%.

**Ethyl 6-chloro-4'-(4-chlorophenyl)-2'-cyclohexyl-2-oxo-2',4'-dihydrospiro [indoline-3,3'-pyrazole] -5'-carboxylate (2j):** 6-Chloro-3-(4-chlorobenzylidene)indolin-2-one (**4c**) (104 mg, 0.358 mmol, 1.0 eq.) and ethyl 2-chloro-2-(2-cyclohexylhydrazono)acetate (**5a**) (125 mg, 0.538 mmol, 1.5 eq.) were added to a pressure tube, under nitrogen atmosphere. MeCN (2.0 mL) was added at room temperature, followed by Et<sub>3</sub>N (150  $\mu$ L, 1.08 mmol, 3.0 eq.). The reaction mixture was stirred at 90 °C for 15 h and then concentrated *in vacuo*. The crude residue was purified by silica gel flash chromatography (elution with CH<sub>2</sub>Cl<sub>2</sub>) to yield the title compound (82 mg, 0.168 mmol, 47%). The compound was recrystallized in Et<sub>2</sub>O/*n*-heptane resulting in a pale-yellow solid; R<sub>f</sub> 0.60 (5% MeOH in CH<sub>2</sub>Cl<sub>2</sub>); m.p.: 212–214 °C; <sup>1</sup>H NMR (300 MHz, CDCl<sub>3</sub>)  $\delta$ <sub>H</sub> 8.29 (s, 1H, NH), 7.19 (d, *J* = 8.49 Hz, 2H, ArH), 6.88–6.76 (m, 3H, ArH), 6.69 (dd, *J* = 8.1, 1.8 Hz, 1H, ArH), 6.28 (d, *J* = 8.1 Hz, 1H, ArH), 4.77 (s, 1H, CH), 4.25–4.12 (m, 2H, CH<sub>2</sub>CH<sub>3</sub>), 2.00–1.90 (m, 1H, CH<sub>2</sub>), 1.87–1.59 (m, 6H, CH<sub>2</sub>), 1.56–1.48 (m, 1H, CH<sub>2</sub>), 1.18 (t, *J* = 7.1 Hz, 3H, CH<sub>2</sub>CH<sub>3</sub>), 1.12–1.00 (m, 2H, CH<sub>2</sub>); <sup>13</sup>C NMR (75 MHz; CDCl<sub>3</sub>)  $\delta$ <sub>C</sub> 177.8 (C=O), 161.7 (C=OOCH<sub>2</sub>CH<sub>3</sub>), 141.5 (Cq), 136.3 (Cq), 135.7 (C=N), 133.7 (Cq), 133.2 (Cq), 129.7 (ArCH), 128.7 (ArCH), 127.4 (ArCH), 122.6 (ArCH), 122.4 (Cq), 111.0 (ArCH), 78.1 (Cq-spiro), 60.9 (CH<sub>2</sub>CH<sub>3</sub>), 59.1 (CH-cyclohexyl), 58.6 (CH), 33.0 (CH<sub>2</sub>), 32.3 (CH<sub>2</sub>), 25.4 (CH<sub>2</sub>), 25.0 (CH<sub>2</sub>), 14.2 (CH<sub>2</sub>CH<sub>3</sub>); LRMS m/z (ESI<sup>+</sup>) [Found: 486, C<sub>25</sub>H<sub>25</sub>Cl<sub>2</sub>N<sub>3</sub>O<sub>3</sub> requires [M+H]<sup>+</sup> 486]; HPLC Method 1 (A): Retention time 10.7 min, 95.0%.

**Ethyl 2'-(tert-butyl)-6-chloro-4'-(4-chlorophenyl)-2-oxo-2',4'-dihydrospiro [indoline-3,3'-pyrazole] -5'-carboxylate (2k):** 6-Chloro-3-(4-chlorobenzylidene)indolin-2-one (**4c**) (202 mg, 0.696 mmol, 1.0 eq.) and ethyl 2-(2-(tert-butyl)hydrazono)-2-chloroacetate (**5b**) (216 mg, 1.04 mmol, 1.5 eq.) were added to a pressure tube, under nitrogen atmosphere. MeCN (3.8 mL) was added at room temperature, followed by Et<sub>3</sub>N (291  $\mu$ L, 2.09 mmol, 3.0 eq.). The reaction mixture was stirred at 90 °C for 15 h and then concentrated *in vacuo*. The crude residue was purified by silica gel flash chromatography (elution with CH<sub>2</sub>Cl<sub>2</sub>) to yield the title compound (196 mg, 0.426 mmol, 61%). The compound was recrystallized in Et<sub>2</sub>O/*n*-heptane resulting in a white solid; R<sub>f</sub> 0.60 (5% MeOH in CH<sub>2</sub>Cl<sub>2</sub>); m.p.: 225–227 °C; <sup>1</sup>H NMR (300 MHz, CDCl<sub>3</sub>)  $\delta$ <sub>H</sub> 8.93 (s, 1H, NH), 7.12 (d, *J* = 8.1 Hz, 2H, ArH), 6.84–6.77 (m, 3H, ArH), 6.74–6.69 (d, *J* = 7.47 Hz, 1H, ArH), 6.50 (d, *J* = 8.1 Hz, 1H, ArH), 4.85 (s, 1H, CH), 4.22–4.10 (m, 2H, CH<sub>2</sub>CH<sub>3</sub>), 1.23 (s, 9H, C(CH<sub>3</sub>)<sub>3</sub>), 1.15 (t, *J* = 7.1 Hz, 3H, CH<sub>2</sub>CH<sub>3</sub>); <sup>13</sup>C NMR (75 MHz; CDCl<sub>3</sub>)  $\delta$ <sub>C</sub> 179.0 (C=O), 161.9 (C=OOCH<sub>2</sub>CH<sub>3</sub>), 140.4 (Cq), 135.4 (C=N), 134.5 (Cq), 133.6 (Cq), 133.2 (Cq), 129.7 (ArCH), 128.5

(ArCH), 127.7 (ArCH), 125.0 (Cq), 122.2 (ArCH), 111.3 (ArCH), 78.3 (Cq-spiro), 61.2 (CH), 60.8 (CH<sub>2</sub>CH<sub>3</sub>), 60.6 (C(CH<sub>3</sub>)<sub>3</sub>), 29.6 (C(CH<sub>3</sub>)<sub>3</sub>), 14.1 (CH<sub>2</sub>CH<sub>3</sub>); LRMS m/z (ESI<sup>+</sup>) [Found: 460, C<sub>23</sub>H<sub>23</sub>Cl<sub>2</sub>N<sub>3</sub>O<sub>3</sub> requires [M+H]<sup>+</sup> 460]; HPLC Method 1 (A): Retention time 9.0 min, 99.4%.

**Ethyl 6-chloro-2'-cyclohexyl-4'-(3-fluorophenyl)-2-oxo-2',4'-dihydrospiro [indoline-3,3'-pyrazole] -5'-carboxylate (2l):** 6-Chloro-3-(3-fluorobenzylidene)indolin-2-one (**4d**) (123 mg, 0.449 mmol, 1.0 eq.) and ethyl 2-chloro-2-(2-cyclohexylhydrazono)acetate (**5a**) (157 mg, 0.674 mmol, 1.5 eq.) were added to a pressure tube, under nitrogen atmosphere. MeCN (2.5 mL) was added at room temperature, followed by Et<sub>3</sub>N (188  $\mu$ L, 1.35 mmol, 3.0 eq.). The reaction mixture was stirred at 90 °C for 15 h and then concentrated *in vacuo*. The crude residue was purified by silica gel flash chromatography (elution with CH<sub>2</sub>Cl<sub>2</sub>) to yield the title compound (146 mg, 0.310 mmol, 69%). The compound was recrystallized in Et<sub>2</sub>O/*n*-heptane resulting in a white solid; R<sub>f</sub> 0.52 (5% MeOH in CH<sub>2</sub>Cl<sub>2</sub>); m.p.: 169–171 °C; <sup>1</sup>H NMR (300 MHz, CDCl<sub>3</sub>)  $\delta$ <sub>H</sub> 8.48 (s, 1H, NH), 7.24–7.05 (m, 1H, ArH), 6.96–6.79 (m, 2H, ArH), 6.74–6.57 (m, 3H, ArH), 6.31 (d, *J* = 8.1 Hz, 1H, ArH), 4.79 (s, 1H, CH), 4.33–4.08 (m, 2H, CH<sub>2</sub>CH<sub>3</sub>), 2.81–2.67 (m, 1H, CH-cyclohexyl), 2.02–1.90 (m, 1H, CH<sub>2</sub>), 1.81–1.59 (m, 6H, CH<sub>2</sub>), 1.58–1.48 (m, 1H, CH<sub>2</sub>), 1.18 (t, *J* = 7.1 Hz, 3H, CH<sub>2</sub>CH<sub>3</sub>), 1.13–0.95 (m, 2H, CH<sub>2</sub>); <sup>13</sup>C NMR (75 MHz; CDCl<sub>3</sub>)  $\delta$ <sub>C</sub> 177.9 (C=O), 162.8 (d, *J*<sub>C-F</sub> = 245.31 Hz, C-F), 161.7 (C=OOCH<sub>2</sub>CH<sub>3</sub>), 141.6 (Cq), 137.3 (d, *J* = 7.00 Hz, Cq), 136.0 (Cq), 135.7 (C=N), 130.1 (d, *J* = 8.22 Hz, ArCH), 127.2 (ArCH), 124.1 (d, *J* = 2.68 Hz, ArCH), 122.5 (ArCH), 122.4 (Cq), 115.3 (d, *J* = 21.68 Hz, ArCH), 114.9 (d, *J* = 20.94 Hz, ArCH), 111.1 (ArCH), 78.2 (Cq-spiro), 60.9 (CH<sub>2</sub>CH<sub>3</sub>), 59.1 (CH-cyclohexyl), 58.9 (CH), 33.1 (CH<sub>2</sub>), 32.3 (CH<sub>2</sub>), 25.5 (CH<sub>2</sub>), 25.0 (CH<sub>2</sub>), 14.1 (CH<sub>2</sub>CH<sub>3</sub>); LRMS m/z (ESI<sup>+</sup>) [Found: 470, C<sub>25</sub>H<sub>25</sub>ClFN<sub>3</sub>O<sub>3</sub> requires [M+H]<sup>+</sup> 470]; HPLC Method 1 (A): Retention time 9.8 min, 99.0%.

**Ethyl 2'-(tert-butyl)-6-chloro-4'-(3-fluorophenyl)-2-oxo-2',4'-dihydrospiro [indoline-3,3'-pyrazole] -5'-carboxylate (2m):** 6-Chloro-3-(3-fluorobenzylidene)indolin-2-one (**4d**) (150 mg, 0.548 mmol, 1.0 eq.) and ethyl 2-(2-(tert-butyl)hydrazono)-2-chloroacetate (**5b**) (170 mg, 0.822 mmol, 1.5 eq.) were added to a pressure tube, under nitrogen atmosphere. MeCN (3.1 mL) was added at room temperature, followed by Et<sub>3</sub>N (229  $\mu$ L, 1.64 mmol, 3.0 eq.). The reaction mixture was stirred at 90 °C for 15 h and then concentrated *in vacuo*. The crude residue was purified by silica gel flash chromatography (elution with CH<sub>2</sub>Cl<sub>2</sub>) to yield the title compound (204 mg, 0.460 mmol, 84%). The compound was recrystallized in Et<sub>2</sub>O/*n*-heptane resulting in a white solid; R<sub>f</sub> 0.50 (5% MeOH in CH<sub>2</sub>Cl<sub>2</sub>); m.p.: 221–222 °C; <sup>1</sup>H NMR (300 MHz, CDCl<sub>3</sub>)  $\delta$ <sub>H</sub> 8.56 (s, 1H, NH), 7.11 (td, *J* = 8.0, 5.9 Hz, 1H, ArH), 6.84 (tdd, *J* = 8.4, 2.6, 1.0 Hz, 1H, ArH), 6.79 (d, *J* = 1.8 Hz, 1H, ArH), 6.71–6.63 (m, 2H, ArH), 6.60 (dt, *J* = 9.7, 2.2 Hz, 1H, ArH), 6.54 (d, *J* = 8.1 Hz, 1H, ArH), 4.88 (s, 1H, CH), 4.24–4.11 (m, 2H, CH<sub>2</sub>CH<sub>3</sub>), 1.24 (s, 9H, C(CH<sub>3</sub>)<sub>3</sub>), 1.15 (t, *J* = 7.1 Hz, 3H, CH<sub>2</sub>CH<sub>3</sub>); <sup>13</sup>C NMR (75 MHz; CDCl<sub>3</sub>)  $\delta$ <sub>C</sub> 178.8 (C=O), 162.6 (d, *J*<sub>C-F</sub> = 245.09 Hz, C-F), 161.8 (C=OOCH<sub>2</sub>CH<sub>3</sub>), 140.1 (Cq), 137.1 (d, *J* = 7.04 Hz, Cq), 135.3 (C=N), 134.2 (Cq), 129.8 (d, *J* = 8.31 Hz, ArCH), 127.6 (ArCH), 125.0 (Cq), 124.1 (d, *J* = 2.75 Hz, ArCH), 122.2 (ArCH), 115.3 (d, *J* = 21.74 Hz, ArCH), 114.7 (d, *J* = 20.89 Hz, ArCH), 111.0 (ArCH), 78.2 (Cq-spiro), 61.6 (CH), 60.7 (CH<sub>2</sub>CH<sub>3</sub>), 60.5 (C(CH<sub>3</sub>)<sub>3</sub>), 29.6 (C(CH<sub>3</sub>)<sub>3</sub>), 14.1 (CH<sub>2</sub>CH<sub>3</sub>); LRMS m/z (ESI<sup>+</sup>) [Found: 444, C<sub>23</sub>H<sub>23</sub>ClFN<sub>3</sub>O<sub>3</sub> requires [M+H]<sup>+</sup> 444]; HPLC Method 1 (A): Retention time 8.9 min, 99.4%.

**Ethyl 6-chloro-4'-(3-fluorophenyl)-2-oxo-2'-phenyl-2',4'-dihydrospiro [indoline-3,3'-pyrazole] -5'-carboxylate (2n):** 6-Chloro-3-(3-fluorobenzylidene)indolin-2-one (**4d**) (120 mg, 0.439 mmol, 1.0 eq.) and ethyl 2-chloro-2-(2-phenylhydrazono)acetate (**5c**) (149 mg, 0.658 mmol, 1.5 eq.) were added to a pressure tube, under nitrogen atmosphere. MeCN (2.5 mL) was added at room temperature, followed by Et<sub>3</sub>N (183  $\mu$ L, 1.32 mmol, 3.0 eq.). The reaction mixture was stirred at 90 °C for 15 h and then concentrated *in vacuo*. The crude residue was purified by silica gel flash chromatography (elution with CH<sub>2</sub>Cl<sub>2</sub>) to yield the title compound (22 mg, 0.047 mmol, 11%). The compound was recrystallized in Et<sub>2</sub>O/*n*-heptane resulting in a yellow solid; R<sub>f</sub> 0.57 (5%

MeOH in  $\text{CH}_2\text{Cl}_2$ ; m.p.: 222–224 °C;  $^1\text{H}$  NMR (300 MHz,  $\text{CDCl}_3$ )  $\delta_{\text{H}}$  8.37 (s, 1H, NH), 7.24–7.07 (m, 3H, ArH), 6.98–6.87 (m, 4H, ArH), 6.84 (d,  $J = 1.9$  Hz, 1H, ArH), 6.74 (d,  $J = 7.6$  Hz, 1H, ArH), 6.70–6.66 (m, 1H, ArH), 6.63 (dd,  $J = 8.2, 1.8$  Hz, 1H, ArH), 6.36 (d,  $J = 8.2$  Hz, 1H, ArH), 5.06 (s, 1H, CH), 4.33–4.22 (m, 2H,  $\text{CH}_2\text{CH}_3$ ), 1.25 (t,  $J = 7.1$  Hz, 3H,  $\text{CH}_2\text{CH}_3$ );  $^{13}\text{C}$  NMR (75 MHz;  $\text{CDCl}_3$ )  $\delta_{\text{C}}$  176.4 (C=O), 162.8 (d,  $J_{\text{C-F}} = 246.26$  Hz, C-F), 161.3 (C=OOC $\text{H}_2\text{CH}_3$ ), 141.6 (Cq), 140.8 (Cq), 140.3 (Cq), 136.6 (d,  $J = 7.16$  Hz, Cq), 136.0 (C=N), 130.3 (d,  $J = 8.21$  Hz, ArCH), 129.1 (ArCH), 127.3 (ArCH), 124.1 (d,  $J = 2.60$  Hz, ArCH), 123.3 (ArCH), 122.8 (ArCH), 122.3 (Cq), 116.5 (ArCH), 115.5 (d,  $J = 22.27$  Hz, ArCH), 115.2 (d,  $J = 20.95$  Hz, ArCH), 111.3 (ArCH), 77.2 (Cq-spiro), 61.5 ( $\text{CH}_2\text{CH}_3$ ), 60.9 (CH), 14.1 ( $\text{CH}_2\text{CH}_3$ ); LRMS  $m/z$  ( $\text{ESI}^+$ ) [Found: 464,  $\text{C}_{25}\text{H}_{19}\text{ClFN}_3\text{O}_3$  requires  $[\text{M}+\text{H}]^+$  464]; HPLC Method 1 (A): Retention time 9.0 min, 96.0%.

**Ethyl 6-chloro-2'-cyclohexyl-4'-(4-fluorophenyl)-2-oxo-2',4'-dihydrospiro[indoline-3,3'-pyrazole]-5'-carboxylate (2o):** 6-Chloro-3-(4-fluorobenzylidene)indolin-2-one (**4e**) (121 mg, 0.442 mmol, 1.0 eq.) and ethyl 2-chloro-2-(2-cyclohexylhydrazono)acetate (**5a**) (154 mg, 0.663 mmol, 1.5 eq.) were added to a pressure tube, under nitrogen atmosphere. MeCN (2.5 mL) was added at room temperature, followed by  $\text{Et}_3\text{N}$  (185  $\mu\text{L}$ , 1.33 mmol, 3.0 eq.). The reaction mixture was stirred at 90 °C for 15 h and then concentrated *in vacuo*. The crude residue was purified by silica gel flash chromatography (elution with  $\text{CH}_2\text{Cl}_2$ ) to yield the title compound (158 mg, 0.337 mmol, 76%). The compound was recrystallized in  $\text{Et}_2\text{O}/n$ -heptane resulting in a white solid;  $R_f$  0.59 (5% MeOH in  $\text{CH}_2\text{Cl}_2$ ); m.p.: 194–196 °C;  $^1\text{H}$  NMR (300 MHz,  $(\text{CD}_3)_2\text{CO}$ )  $\delta_{\text{H}}$  9.65 (s, 1H, NH), 7.01 (d,  $J = 7.0$  Hz, 4H, ArH), 6.90 (d,  $J = 1.9$  Hz, 1H, ArH), 6.70 (dd,  $J = 8.0, 2.0$  Hz, 1H, ArH), 6.41 (d,  $J = 8.1$  Hz, 1H, ArH), 4.79 (s, 1H, CH), 4.17–4.07 (m, 2H,  $\text{CH}_2\text{CH}_3$ ), 2.88–2.70 (m, 1H, CH-cyclohexyl), 2.00–1.96 (m, 1H,  $\text{CH}_2$ ), 1.87–1.37 (m, 7H, CH), 1.17–1.08 (t,  $J = 7.1$  Hz, 3H,  $\text{CH}_2\text{CH}_3$ ); br s, 2H,  $\text{CH}_2$ ;  $^{13}\text{C}$  NMR (75 MHz;  $(\text{CD}_3)_2\text{CO}$ )  $\delta_{\text{C}}$  177.8 (C=O), 163.0 (d,  $J_{\text{C-F}} = 243.02$  Hz, C-F), 162.1 (C=OOC $\text{H}_2\text{CH}_3$ ), 144.7 (Cq), 137.5 (C=N), 135.8 (Cq), 132.6 (d,  $J = 3.20$  Hz, Cq), 131.3 (d,  $J = 8.21$  Hz, ArCH), 128.6 (ArCH), 124.0 (Cq), 122.2 (ArCH), 116.0 (d,  $J = 21.52$  Hz, ArCH), 111.3 (ArCH), 78.9 (Cq-spiro), 60.7 ( $\text{CH}_2\text{CH}_3$ ), 59.3 (CH), 59.2 (CH-cyclohexyl), 34.1 ( $\text{CH}_2$ ), 33.2 ( $\text{CH}_2$ ), 26.1 ( $\text{CH}_2$ ), 26.0 ( $\text{CH}_2$ ), 14.5 ( $\text{CH}_2\text{CH}_3$ ); LRMS  $m/z$  ( $\text{ESI}^+$ ) [Found: 470,  $\text{C}_{25}\text{H}_{25}\text{ClFN}_3\text{O}_3$  requires  $[\text{M}+\text{H}]^+$  470]; HPLC Method 1 (A): Retention time 9.9 min, 98.6%.

**Ethyl 2'-(tert-butyl)-6-chloro-4'-(4-fluorophenyl)-2-oxo-2',4'-dihydrospiro[indoline-3,3'-pyrazole]-5'-carboxylate (2p):** 6-Chloro-3-(4-fluorobenzylidene)indolin-2-one (**4e**) (155 mg, 0.567 mmol, 1.0 eq.) and ethyl 2-(2-(tert-butyl)hydrazono)-2-chloroacetate (**5b**) (176 mg, 0.851 mmol, 1.5 eq.) were added to a pressure tube, under nitrogen atmosphere. MeCN (3.1 mL) was added at room temperature, followed by  $\text{Et}_3\text{N}$  (237  $\mu\text{L}$ , 1.70 mmol, 3.0 eq.). The reaction mixture was stirred at 90 °C for 15 h and then concentrated *in vacuo*. The crude residue was purified by silica gel flash chromatography (elution with  $\text{CH}_2\text{Cl}_2$ ) to yield the title compound (189 mg, 0.189 mmol, 75%). The compound was recrystallized in  $\text{Et}_2\text{O}/n$ -heptane resulting in a white solid;  $R_f$  0.42 (5% MeOH in  $\text{CH}_2\text{Cl}_2$ ); m.p.: 187–189 °C;  $^1\text{H}$  NMR (300 MHz,  $\text{CDCl}_3$ )  $\delta_{\text{H}}$  8.40 (s, 1H, NH), 6.84 (d,  $J = 6.9$  Hz, 4H, ArH), 6.77 (d,  $J = 1.9$  Hz, 1H, ArH), 6.68 (dd,  $J = 8.1, 1.8$  Hz, 1H, ArH), 6.50 (d,  $J = 8.1$  Hz, 1H, ArH), 4.87 (s, 1H, CH), 4.23–4.03 (m, 2H,  $\text{CH}_2\text{CH}_3$ ), 1.24 (s, 9H,  $\text{C}(\text{CH}_3)_3$ ), 1.14 (t,  $J = 7.1$  Hz, 3H,  $\text{CH}_2\text{CH}_3$ );  $^{13}\text{C}$  NMR (75 MHz;  $\text{CDCl}_3$ )  $\delta_{\text{C}}$  178.8 (C=O), 162.1 (d,  $J_{\text{C-F}} = 245.24$  Hz, C-F), 161.9 (C=OOC $\text{H}_2\text{CH}_3$ ), 140.0 (Cq), 135.2 (Cq), 134.7 (C=N), 130.4 (d,  $J = 3.26$  Hz, Cq), 129.9 (d,  $J = 8.11$  Hz, ArCH), 127.6 (ArCH), 125.1 (Cq), 122.2 (ArCH) 115.3 (d,  $J = 21.47$  Hz, ArCH), 110.9 (ArCH), 78.2 (Cq-spiro), 61.2 (CH), 60.7 ( $\text{CH}_2\text{CH}_3$ ), 60.4 ( $\text{C}(\text{CH}_3)_3$ ), 29.6 ( $\text{C}(\text{CH}_3)_3$ ), 14.1 ( $\text{CH}_2\text{CH}_3$ ); LRMS  $m/z$  ( $\text{ESI}^+$ ) [Found: 444,  $\text{C}_{23}\text{H}_{23}\text{ClFN}_3\text{O}_3$  requires  $[\text{M}+\text{H}]^+$  444]; HPLC Method 1 (A): Retention time 9.0 min, 95.0%.

**Ethyl 6-chloro-4'-(3-chloro-2-fluorophenyl)-2'-(4-chlorophenyl)-2-oxo-2',4'-dihydrospiro[indoline-3,3'-pyrazole]-5'-carboxylate (2q):** 6-Chloro-3-(3-chloro-2-fluorobenzylidene)indolin-2-one (**4a**) (100 mg, 0.325 mmol, 1.0 eq.) and ethyl 2-chloro-2-(2-(4-chlorophenyl)

hydrazono)acetate (**5d**) (127 mg, 0.487 mmol, 1.5 eq.) were added to a pressure tube, under nitrogen atmosphere. MeCN (1.9 mL) was added at room temperature, followed by  $\text{Et}_3\text{N}$  (136  $\mu\text{L}$ , 0.974 mmol, 3.0 eq.). The reaction mixture was stirred at 90 °C for 15 h and then concentrated *in vacuo*. The crude residue was purified by silica gel flash chromatography (elution with  $\text{CH}_2\text{Cl}_2$ ) to yield the title compound (53 mg, 0.100 mmol, 31%). The compound was recrystallized in  $\text{Et}_2\text{O}/n$ -heptane resulting in a yellow solid;  $R_f$  0.83 (5% MeOH in  $\text{CH}_2\text{Cl}_2$ ); m.p.: 221–223 °C;  $^1\text{H}$  NMR (300 MHz,  $\text{CDCl}_3$ )  $\delta_{\text{H}}$  7.65 (s, 1H, NH), 7.32–7.28 (m, 1H, ArH), 7.16–7.08 (m, 2H, ArH), 7.08–6.95 (m, 2H, ArH), 6.94–6.88 (m, 1H, ArH), 6.88–6.82 (m, 2H, ArH), 6.69 (d,  $J = 1.94$  Hz, 1H, ArH), 6.26 (br s, 1H, ArH), 5.40 (s, 1H, CH), 4.37–4.22 (m, 2H,  $\text{CH}_2\text{CH}_3$ ), 1.28 (t,  $J = 7.1$  Hz, 3H,  $\text{CH}_2\text{CH}_3$ );  $^{13}\text{C}$  NMR (75 MHz;  $\text{CDCl}_3$ )  $\delta_{\text{C}}$  175.7 (C=O), 161.0 (C=OOC $\text{H}_2\text{CH}_3$ ), 155.9 (d,  $J_{\text{C-F}} = 247.8$  Hz, C-F), 140.1 (Cq), 139.3 (Cq), 136.5 (C=N), 130.8 (ArCH), 129.1 (ArCH), 127.0 (ArCH), 126.7 (ArCH), 124.7 (ArCH), 124.6 (Cq), 123.70 (d,  $J = 14.1$  Hz, Cq), 122.8 (ArCH), 122.3 (Cq), 121.8 (Cq), 121.6 (Cq), 117.6 (ArCH), 111.6 (ArCH), 77.2 (Cq-spiro), 61.6 ( $\text{CH}_2\text{CH}_3$ ), 53.8 (CH), 14.1 ( $\text{CH}_2\text{CH}_3$ ); LRMS  $m/z$  ( $\text{ESI}^+$ ) [Found: 534,  $\text{C}_{25}\text{H}_{17}\text{Cl}_3\text{FN}_3\text{O}_3$  requires  $[\text{M}+\text{H}]^+$  534]; HPLC Method 1 (A): Retention time 10.2 min, 100.0%.

**Ethyl 2'-(tert-butyl)-6-chloro-4'-(3-chloro-2-fluorophenyl)-5-fluoro-2-oxo-2',4'-dihydrospiro[indoline-3,3'-pyrazole]-5'-carboxylate (2r):** 6-Chloro-3-(3-chloro-2-fluorobenzylidene)-5-fluoroindolin-2-one (**4f**) (104 mg, 0.319 mmol, 1.0 eq.) and ethyl 2-(2-(tert-butyl)hydrazono)-2-chloroacetate (**5b**) (99 mg, 0.478 mmol, 1.5 eq.) were added to a pressure tube, under nitrogen atmosphere. MeCN (2.0 mL) was added at room temperature, followed by  $\text{Et}_3\text{N}$  (133  $\mu\text{L}$ , 0.957 mmol, 3.0 eq.). The reaction mixture was stirred at 90 °C for 15 h and then concentrated *in vacuo*. The crude residue was purified by silica gel flash chromatography (elution with  $\text{EtOAc}/n$ -hexane 1:3) to yield the title compound (86 mg, 0.174 mmol, 55%). The compound was recrystallized in  $\text{Et}_2\text{O}/n$ -heptane resulting in a white solid;  $R_f$  0.53 (5% MeOH in  $\text{CH}_2\text{Cl}_2$ ); m.p.: 190–191 °C;  $^1\text{H}$  NMR (300 MHz,  $\text{CDCl}_3$ )  $\delta_{\text{H}}$  8.48 (s, 1H, NH), 7.23 (d,  $J = 7.5$  Hz, 1H, ArH), 7.05 (t,  $J = 7.8$  Hz, 1H, ArH), 7.00–6.82 (m, 2H, ArH), 6.24 (d,  $J = 8.1$  Hz, 1H, ArH), 5.23 (s, 1H, CH), 4.32–4.02 (m, 2H,  $\text{CH}_2\text{CH}_3$ ), 1.25 (s, 9H,  $\text{C}(\text{CH}_3)_3$ ), 1.18 (t,  $J = 7.1$  Hz, 3H,  $\text{CH}_2\text{CH}_3$ );  $^{13}\text{C}$  NMR (75 MHz;  $\text{CDCl}_3$ )  $\delta_{\text{C}}$  178.0 (C=O), 161.4 (C=OOC $\text{H}_2\text{CH}_3$ ), 155.9 (d,  $J_{\text{C-F}} = 247.15$  Hz, C-F), 153.6 (d,  $J_{\text{C-F}} = 243.59$  Hz, C-F), 136.4 (Cq), 132.8 (C=N), 130.4 (ArCH), 127.4 (ArCH), 126.6 (d,  $J = 7.07$  Hz, Cq), 124.4 (d,  $J = 4.61$  Hz, ArCH), 124.1 (d,  $J = 15.29$  Hz, Cq), 122.3 (d,  $J = 19.51$  Hz, Cq), 121.3 (d,  $J = 18.32$  Hz, Cq), 114.7 (d,  $J = 25.95$  Hz, ArCH), 112.3 (ArCH), 77.2 (Cq-spiro), 60.9 ( $\text{CH}_2\text{CH}_3$ ), 60.8 ( $\text{C}(\text{CH}_3)_3$ ), 54.4 (d,  $J = 1.73$  Hz, CH), 29.5 ( $\text{C}(\text{CH}_3)_3$ ), 14.1 ( $\text{CH}_2\text{CH}_3$ ); LRMS  $m/z$  ( $\text{ESI}^+$ ) [Found: 496,  $\text{C}_{23}\text{H}_{21}\text{Cl}_2\text{F}_2\text{N}_3\text{O}_3$  requires  $[\text{M}+\text{H}]^+$  496]; HPLC Method 1 (A): Retention time 9.4 min, 99.6%.

**Ethyl 2'-(tert-butyl)-6-chloro-5-fluoro-4'-(3-fluorophenyl)-2-oxo-2',4'-dihydrospiro[indoline-3,3'-pyrazole]-5'-carboxylate (2s):** 6-Chloro-5-fluoro-3-(3-fluorobenzylidene)indolin-2-one (**4g**) (106 mg, 0.363 mmol, 1.0 eq.) and ethyl 2-(2-(tert-butyl)hydrazono)-2-chloroacetate (**5b**) (113 mg, 0.545 mmol, 1.5 eq.) were added to a pressure tube, under nitrogen atmosphere. MeCN (2.0 mL) was added at room temperature, followed by  $\text{Et}_3\text{N}$  (152  $\mu\text{L}$ , 1.09 mmol, 3.0 eq.). The reaction mixture was stirred at 90 °C for 15 h and then concentrated *in vacuo*. The crude residue was purified by silica gel flash chromatography (elution with  $\text{EtOAc}/n$ -hexane 1:3) to yield the title compound (84 mg, 0.181 mmol, 50%). The compound was recrystallized in  $\text{Et}_2\text{O}/n$ -heptane resulting in a white solid;  $R_f$  0.42 (5% MeOH in  $\text{CH}_2\text{Cl}_2$ ); m.p.: 216–217 °C;  $^1\text{H}$  NMR (300 MHz,  $\text{CDCl}_3$ )  $\delta_{\text{H}}$  8.35 (s, 1H, NH), 7.16 (td,  $J = 8.1, 5.9$  Hz, 1H, ArH), 6.88 (tdd,  $J = 8.4, 2.6, 1.0$  Hz, 1H, ArH), 6.82 (d,  $J = 5.9$  Hz, 1H, ArH), 6.67 (d,  $J = 7.5$  Hz, 1H, ArH), 6.60 (dt,  $J = 9.7, 2.4$  Hz, 1H, ArH), 6.41 (d,  $J = 8.3$  Hz, 1H, ArH), 4.88 (s, 1H, CH), 4.30–3.94 (m, 2H,  $\text{CH}_2\text{CH}_3$ ), 1.26 (s, 9H,  $\text{C}(\text{CH}_3)_3$ ), 1.16 (t,  $J = 7.1$  Hz, 3H,  $\text{CH}_2\text{CH}_3$ );  $^{13}\text{C}$  NMR (75 MHz;  $\text{CDCl}_3$ )  $\delta_{\text{C}}$  178.5 (C=O), 162.7 (d,  $J_{\text{C-F}} = 246.00$  Hz, C-F), 161.6 (C=OOC $\text{H}_2\text{CH}_3$ ), 153.8 (d,  $J_{\text{C-F}} = 243.53$  Hz, C-F), 136.7 (d,  $J = 6.75$  Hz, Cq), 135.5 (d,  $J = 1.50$  Hz, Cq), 134.6 (C=N), 130.1 (d,  $J = 8.25$  Hz, ArCH), 126.7 (d,  $J = 6.75$  Hz, Cq), 124.0 (d,  $J = 3.00$  Hz,

ArCH), 122.0 (d,  $J = 19.50$  Hz, Cq), 115.3 (d,  $J = 4.5$  Hz, ArCH), 115.1 (d,  $J = 21.00$  Hz, ArCH), 115.0 (ArCH), 112.1 (ArCH), 78.1 (d,  $J = 1.18$  Hz, Cq-spiro), 61.7 (d,  $J = 0.75$  Hz, CH), 60.9 (CH<sub>2</sub>CH<sub>3</sub>), 60.6 (C(CH<sub>3</sub>)<sub>3</sub>), 29.6 (C(CH<sub>3</sub>)<sub>3</sub>), 14.1 (CH<sub>2</sub>CH<sub>3</sub>); LRMS  $m/z$  (ESI<sup>+</sup>) [Found: 462, C<sub>23</sub>H<sub>22</sub>ClF<sub>2</sub>N<sub>3</sub>O<sub>3</sub> requires [M+H]<sup>+</sup> 462]; HPLC Method 1 (A): Retention time 8.9 min, 99.8%.

**Ethyl 6-chloro-2'-(4-chlorophenyl)-4'-(3-hydroxyphenyl)-2-oxo-2',4'-dihydrospiro [indoline-3,3'-pyrazole]-5'-carboxylate (3a):** 6-Chloro-3-(3-hydroxybenzylidene)indolin-2-one (4h) (50 mg, 0.184 mmol, 1.0 eq.) and ethyl 2-chloro-2-(2-(4-chlorophenyl)hydrazono)acetate (5d) (72 mg, 0.276 mmol, 1.5 eq.) were added to a pressure tube, under nitrogen atmosphere. MeCN (1.0 mL) was added at room temperature, followed by Et<sub>3</sub>N (77  $\mu$ L, 0.552 mmol, 3.0 eq.). The reaction mixture was stirred at 90 °C for 15 h and then concentrated *in vacuo*. The crude residue was purified by silica gel flash chromatography (elution with 5% MeOH in CH<sub>2</sub>Cl<sub>2</sub>) to yield the title compound (51 mg, 0.101 mmol, 55%). The compound was recrystallized in Et<sub>2</sub>O/*n*-heptane resulting in a yellow solid;  $R_f$  0.28 (5% MeOH in CH<sub>2</sub>Cl<sub>2</sub>); m.p.: 224–226 °C; <sup>1</sup>H NMR (300 MHz, (CD<sub>3</sub>)<sub>2</sub>CO)  $\delta_H$  8.56 (s, 1H, NH), 7.08–7.00 (m, 3H, ArH), 6.82–6.78 (m, 2H, ArH), 6.77 (d,  $J = 1.9$  Hz, 1H, ArH), 6.70–6.64 (m, 1H, ArH), 6.61 (dd,  $J = 8.2, 1.8$  Hz, 1H, ArH), 6.48–6.42 (m, 2H, ArH), 6.35 (d,  $J = 8.2$  Hz, 1H, ArH), 4.99 (s, 1H, CH), 4.26–4.23 (m, 2H, CH<sub>2</sub>CH<sub>3</sub>), 1.22 (t,  $J = 7.1$  Hz, 3H, CH<sub>2</sub>CH<sub>3</sub>); <sup>13</sup>C NMR (75 MHz, (CD<sub>3</sub>)<sub>2</sub>CO)  $\delta_C$  176.4 (C=O), 161.7 (C=OCH<sub>2</sub>CH<sub>3</sub>), 158.6 (C–OH), 143.9 (Cq), 143.0 (Cq), 142.2 (Cq), 136.8 (C=N), 136.1 (Cq), 130.5 (ArCH), 129.8 (ArCH), 128.4 (ArCH), 127.9 (Cq), 123.5 (Cq), 122.6 (ArCH), 120.5 (ArCH), 118.1 (ArCH), 116.3 (ArCH), 116.0 (ArCH), 111.7 (ArCH), 77.6 (Cq-spiro), 62.1 (CH), 61.6 (CH<sub>2</sub>CH<sub>3</sub>), 14.4 (CH<sub>2</sub>CH<sub>3</sub>); LRMS  $m/z$  (ESI<sup>+</sup>) [Found: 496, C<sub>25</sub>H<sub>19</sub>Cl<sub>2</sub>N<sub>3</sub>O<sub>3</sub> requires [M+H]<sup>+</sup> 496]; HPLC Method 1 (A): Retention time 9.6 min, 98.0%.

#### 4.1.2. General procedure for the hydrolysis of spiroprazolone oxindoles (2b and 2d)

To a solution of spiroprazolone oxindole (1.0 eq.) in THF/MeOH/H<sub>2</sub>O (1:1:1) (6.5 mL/mmol) was added sodium hydroxide (5.0 eq.). The reaction mixture was stirred at 50 °C, controlled by TLC until total consumption of spiroprazolone oxindole, and then diluted with H<sub>2</sub>O. The solution was neutralized with aqueous 1 M HCl and extracted several times with EtOAc. The combined organic extracts were dried over Na<sub>2</sub>SO<sub>4</sub>, filtered, and concentrated *in vacuo* to yield the carboxylic acid of the spiroprazolone oxindole without further purification.

**6-Chloro-4'-(3-chloro-2-fluorophenyl)-2'-cyclohexyl-2-oxo-2',4'-dihydrospiro [indoline-3,3'-pyrazole]-5'-carboxylic acid (2b):** To a solution of ethyl 6-chloro-4'-(3-chloro-2-fluorophenyl)-2'-cyclohexyl-2-oxo-2',4'-dihydrospiro[indoline-3,3'-pyrazole]-5'-carboxylate (2a) (283 mg, 0.561 mmol, 1.0 eq.) in THF/MeOH/H<sub>2</sub>O (1:1:1) (3.3 mL) was added sodium hydroxide (112 mg, 2.81 mmol, 5.0 eq.). The reaction mixture was stirred at 50 °C for 5 h and then diluted with H<sub>2</sub>O (8 mL). The solution was neutralized with aqueous 1 M HCl and extracted several times with EtOAc (8 mL). The combined organic extracts were dried over Na<sub>2</sub>SO<sub>4</sub>, filtered, and concentrated *in vacuo* to yield the title compound as a white solid (244 mg, 0.513 mmol, 92%) which was used for the next reaction without further purification;  $R_f$  0.00 (5% MeOH in CH<sub>2</sub>Cl<sub>2</sub>); m.p.: 231–232 °C; <sup>1</sup>H NMR (300 MHz, (CD<sub>3</sub>)<sub>2</sub>SO)  $\delta_H$  10.94 (s, 1H, COOH), 7.45 (t,  $J = 7.4$  Hz, 1H, ArH), 7.32–7.14 (m, 1H, ArH), 7.00 (t,  $J = 7.3$  Hz, 1H, ArH), 6.87 (s, 1H, ArH), 6.71 (d,  $J = 8.1$  Hz, 1H, ArH), 6.24 (d,  $J = 8.0$  Hz, 1H, ArH), 4.83 (s, 1H, CH), 2.72–2.57 (m, 1H, CH<sub>2</sub>), 1.72–1.38 (m, 6H, CH<sub>2</sub>), 1.11–0.94 (m, 2H, CH<sub>2</sub>); LRMS  $m/z$  (ESI<sup>+</sup>) [Found: 476, C<sub>23</sub>H<sub>20</sub>Cl<sub>2</sub>FN<sub>3</sub>O<sub>3</sub> requires [M+H]<sup>+</sup> 476]; HPLC Method 1 (A): Retention time 6.2 min, 99.6%.

**2'-(tert-Butyl)-6-chloro-4'-(3-chloro-2-fluorophenyl)-2-oxo-2',4'-dihydrospiro [indoline-3,3'-pyrazole]-5'-carboxylic acid (2d):** To a solution of ethyl 2'-(tert-butyl)-6-chloro-4'-(3-chloro-2-fluorophenyl)-2-oxo-2',4'-dihydrospiro[indoline-3,3'-pyrazole]-5'-carboxylate (2c) (370 mg, 0.774 mmol, 1.0 eq.) in THF/MeOH/H<sub>2</sub>O (1:1:1) (5 mL) was added sodium hydroxide (155 mg, 3.87 mmol, 5.0 eq.). The

reaction mixture was stirred at 50 °C for 5 h and then diluted with H<sub>2</sub>O (10 mL). The solution was neutralized with aqueous 1 M HCl and extracted several times with EtOAc (10 mL). The combined organic extracts were dried over Na<sub>2</sub>SO<sub>4</sub>, filtered, and concentrated *in vacuo* to yield the title compound as a white solid (337 mg, 0.748 mmol, 97%) which was used for the next reaction without further purification;  $R_f$  0.00 (5% MeOH in CH<sub>2</sub>Cl<sub>2</sub>); m.p.: 235–238 °C; <sup>1</sup>H NMR (300 MHz, (CD<sub>3</sub>)<sub>2</sub>SO)  $\delta_H$  9.75 (s, 1H, COOH), 7.21 (t,  $J = 7.6$  Hz, 1H, ArH), 7.14–6.91 (m, 2H, ArH), 6.80 (s, 1H, ArH), 6.58 (d,  $J = 8.0$  Hz, 1H, ArH), 6.42 (d,  $J = 8.1$  Hz, 1H, ArH), 4.97 (s, 1H, CH), 1.10 (s, 9H, C(CH<sub>3</sub>)<sub>3</sub>); LRMS  $m/z$  (ESI<sup>+</sup>) [Found: 450, C<sub>21</sub>H<sub>18</sub>Cl<sub>2</sub>FN<sub>3</sub>O<sub>3</sub> requires [M+H]<sup>+</sup> 450]; HPLC Method 1 (A): Retention time 6.0 min, 95.0%.

#### 4.1.3. General procedure for the synthesis of spiroprazolone oxindole amide derivatives (2e-g)

To a solution of spiroprazolone oxindole 2d (1.0 eq.) in anhydrous DMF (6.8 mL/mmol of acid) was added DIPEA, (2.0 eq.), HOBt (1.5 eq.) and TBTU (1.5 eq.) at room temperature. The reaction mixture was stirred at room temperature for 15 min. The appropriate amine (1.1 eq.) in DMF (4.6 mL/mmol amine) was added to the previous flask. The reaction mixture was stirred at room temperature for 18–21 h. After that time, the reaction mixture was diluted with H<sub>2</sub>O and extracted with EtOAc. The combined organic phases were washed with H<sub>2</sub>O, brine, dried over Na<sub>2</sub>SO<sub>4</sub>, filtered, and concentrated *in vacuo*. The crude residue was purified by silica gel flash chromatography to yield the title spiroprazolone oxindole amide derivative.

**2'-(tert-Butyl)-6-chloro-4'-(3-chloro-2-fluorophenyl)-N-(2-hydroxyethyl)-2-oxo-2',4'-dihydrospiro [indoline-3,3'-pyrazole]-5'-carboxamide (2e):** To a solution of 2'-(tert-butyl)-6-chloro-4'-(3-chloro-2-fluorophenyl)-2-oxo-2',4'-dihydrospiro[indoline-3,3'-pyrazole]-5'-carboxylic acid (2d) (28 mg, 0.062 mmol, 1.0 eq.) in anhydrous DMF (0.4 mL) was added DIPEA (22  $\mu$ L, 0.124 mmol, 2.0 eq.), HOBt (13 mg, 0.093 mmol, 1.5 eq.) and TBTU (30 mg, 0.093 mmol, 1.5 eq.). The reaction mixture was stirred at room temperature for 15 min 2-Aminoethan-1-ol (4  $\mu$ L, 0.068 mmol, 1.1 eq.) in DMF (0.3 mL) was added to the previous flask, and the reaction was stirred at room temperature for 18 h. After that time, the reaction mixture was diluted with H<sub>2</sub>O (5 mL) and extracted with EtOAc (3  $\times$  2 mL). The combined organic phases were washed with H<sub>2</sub>O, brine, dried over Na<sub>2</sub>SO<sub>4</sub>, filtered, and concentrated *in vacuo*. The crude residue was purified by silica gel flash chromatography (elution with 5% MeOH in CH<sub>2</sub>Cl<sub>2</sub>) to yield the title compound as a white foam (14 mg, 0.028 mmol, 46%);  $R_f$  0.18 (5% MeOH in CH<sub>2</sub>Cl<sub>2</sub>); m.p.: 185–187 °C; <sup>1</sup>H NMR (300 MHz, (CD<sub>3</sub>)<sub>2</sub>CO)  $\delta_H$  9.82 (s, 1H, NH), 7.59 (br s, 1H, NHCO), 7.39–7.27 (m, 1H, ArH), 7.23–7.02 (m, 2H, ArH), 6.92 (s, 1H, ArH), 6.69 (d,  $J = 8.0$  Hz, 1H, ArH), 6.47 (d,  $J = 8.1$  Hz, 1H, ArH), 5.10 (s, 1H, CH), 3.95 (t,  $J = 5.2$  Hz, 1H, OH), 3.69–3.60 (m, 2H, CH<sub>2</sub>CH<sub>2</sub>OH), 3.44–3.35 (m, 2H, CH<sub>2</sub>CH<sub>2</sub>OH), 1.20 (s, 9H, C(CH<sub>3</sub>)<sub>3</sub>); <sup>13</sup>C NMR (75 MHz; (CD<sub>3</sub>)<sub>2</sub>CO)  $\delta_C$  178.4 (C=O), 162.1 (C=ONH), 156.5 (d,  $J_{C-F} = 243.75$  Hz, C–F), 145.0 (Cq), 143.5 (Cq), 138.1 (Cq), 135.5 (C=N), 130.6 (ArCH), 129.2 (ArCH), 128.3 (ArCH), 126.8 (Cq), 126.0 (d,  $J = 14.24$  Hz, Cq), 125.5 (d,  $J = 4.36$  Hz, ArCH), 121.8 (ArCH), 111.3 (ArCH), 77.4 (Cq-spiro), 61.9 (CH<sub>2</sub>CH<sub>2</sub>OH), 60.4 (C(CH<sub>3</sub>)<sub>3</sub>), 54.8 (CH), 42.6 (CH<sub>2</sub>CH<sub>2</sub>OH), 29.4 (C(CH<sub>3</sub>)<sub>3</sub>); LRMS  $m/z$  (ESI<sup>+</sup>) [Found: 493, C<sub>23</sub>H<sub>23</sub>Cl<sub>2</sub>FN<sub>3</sub>O<sub>3</sub> requires [M+H]<sup>+</sup> 493]; HPLC Method 1 (A): Retention time 6.9 min, 98.1%.

**2'-(tert-Butyl)-6-chloro-4'-(3-chloro-2-fluorophenyl)-N-(4-hydroxyphenethyl)-2-oxo-2',4'-dihydrospiro [indoline-3,3'-pyrazole]-5'-carboxamide (2f):** To a solution of 2'-(tert-butyl)-6-chloro-4'-(3-chloro-2-fluorophenyl)-2-oxo-2',4'-dihydrospiro[indoline-3,3'-pyrazole]-5'-carboxylic acid (2d) (28 mg, 0.062 mmol, 1.0 eq.) in anhydrous DMF (0.4 mL) was added DIPEA (22  $\mu$ L, 0.124 mmol, 2.0 eq.), HOBt (13 mg, 0.093 mmol, 1.5 eq.) and TBTU (30 mg, 0.093 mmol, 1.5 eq.). The reaction mixture was stirred at room temperature for 15 min 4-(2-Aminoethyl)phenol (9 mg, 0.068 mmol, 1.1 eq.) in DMF (0.3 mL) was added to the previous flask, and the reaction was stirred at room temperature for 18 h. After that time, the reaction mixture was

diluted with H<sub>2</sub>O (5 mL) and extracted with EtOAc (3 × 2 mL). The combined organic phases were washed with H<sub>2</sub>O, brine, dried over Na<sub>2</sub>SO<sub>4</sub>, filtered, and concentrated *in vacuo*. The crude residue was purified by silica gel flash chromatography (elution with 5% MeOH in CH<sub>2</sub>Cl<sub>2</sub>) to yield the title compound as a white foam (16 mg, 0.028 mmol, 45%); R<sub>f</sub> 0.05 (5% MeOH in CH<sub>2</sub>Cl<sub>2</sub>); m.p.: 179–181 °C; <sup>1</sup>H NMR (300 MHz, (CD<sub>3</sub>)<sub>2</sub>CO) δ<sub>H</sub> 9.79 (br s, 1H, OH), 8.14 (br s, 1H, NH), 7.50 (br s, 1H, NHCO), 7.31 (t, *J* = 7.7 Hz, 1H, ArH), 7.15 (t, *J* = 7.9 Hz, 1H, ArH), 7.10–7.02 (m, 2H, ArH), 6.97 (t, *J* = 7.1 Hz, 1H, ArH), 6.90 (s, 1H, ArH), 6.81–6.74 (m, 2H, ArH), 6.68 (d, *J* = 8.0 Hz, 1H, ArH), 6.44 (d, *J* = 8.2 Hz, 1H, ArH), 5.09 (s, 1H, CH), 3.54–3.36 (m, 2H, CH<sub>2</sub>CH<sub>2</sub>PhOH), 2.80–2.70 (m, 2H, CH<sub>2</sub>CH<sub>2</sub>PhOH), 1.19 (s, 9H, C(CH<sub>3</sub>)<sub>3</sub>); <sup>13</sup>C NMR (75 MHz; (CD<sub>3</sub>)<sub>2</sub>CO) δ<sub>C</sub> 178.4 (C=O), 161.5 (C=ONH), 156.7 (Cq), 156.5 (d, *J*<sub>C-F</sub> = 245.84 Hz, C-F), 143.5 (Cq), 138.3 (Cq), 135.5 (C=N), 131.0 (Cq), 130.6 (ArCH), 129.3 (ArCH), 128.3 (ArCH), 126.8 (Cq), 125.9 (d, *J* = 14.86 Hz, Cq), 125.5 (ArCH), 125.5 (ArCH), 121.8 (ArCH), 116.0 (ArCH), 111.2 (ArCH), 78.5 (Cq-spiro), 60.3 (C(CH<sub>3</sub>)<sub>3</sub>), 54.9 (CH), 41.5 (CH<sub>2</sub>CH<sub>2</sub>PhOH), 35.7 (CH<sub>2</sub>CH<sub>2</sub>PhOH), 29.5 (C(CH<sub>3</sub>)<sub>3</sub>); LRMS *m/z* (ESI<sup>+</sup>) [Found: 569, C<sub>29</sub>H<sub>27</sub>Cl<sub>2</sub>FN<sub>4</sub>O<sub>3</sub> requires [M+H]<sup>+</sup> 569]; HPLC Method 1 (A): Retention time 8.1 min, 98.7%.

**2'-(*tert*-Butyl)-6-chloro-4'-(3-chloro-2-fluorophenyl)-*N*-(4-hydroxyphenyl)-2-oxo-2',4'-dihydrospiro [indoline-3,3'-pyrazole]-5'-carboxamide (2g):** To a solution of 2'-(*tert*-butyl)-6-chloro-4'-(3-chloro-2-fluorophenyl)-2-oxo-2',4'-dihydrospiro[indoline-3,3'-pyrazole]-5'-carboxylic acid (**2d**) (28 mg, 0.062 mmol, 1.0 eq.) in anhydrous DMF (0.4 mL) was added DIPEA (22 μL, 0.124 mmol, 2.0 eq.), HOBt (13 mg, 0.093 mmol, 1.5 eq.) and TBTU (30 mg, 0.093 mmol, 1.5 eq.). The reaction mixture was stirred at room temperature for 15 min. 4-Aminophenol (8 mg, 0.068 mmol, 1.1 eq.) in DMF (0.3 mL) was added to the previous flask, and the reaction was stirred at room temperature for 22 h. The reaction mixture was diluted with H<sub>2</sub>O (5 mL) and extracted with EtOAc (3 × 2 mL). The combined organic phases were washed with H<sub>2</sub>O, brine, dried over Na<sub>2</sub>SO<sub>4</sub>, filtered, and concentrated *in vacuo*. The crude residue was purified by silica gel flash chromatography (elution with 5% MeOH in CH<sub>2</sub>Cl<sub>2</sub>) to yield the title compound as a white foam (14 mg, 0.026 mmol, 42%); R<sub>f</sub> 0.10 (5% MeOH in CH<sub>2</sub>Cl<sub>2</sub>); m.p.: 193–195 °C; <sup>1</sup>H NMR (300 MHz, (CD<sub>3</sub>)<sub>2</sub>CO) δ<sub>H</sub> 9.28 (br s, 1H, OH), 7.52–7.47 (m, 2H, ArH), 7.36–7.31 (m, 1H, ArH), 7.23–7.07 (m, 2H, ArH), 6.87 (s, 1H, ArH), 6.76–6.67 (m, 3H, ArH), 6.49 (d, *J* = 7.8 Hz, 1H, ArH), 5.13 (s, 1H, CH), 1.23 (s, 9H, C(CH<sub>3</sub>)<sub>3</sub>); <sup>13</sup>C NMR (75 MHz; (CD<sub>3</sub>)<sub>2</sub>CO) δ<sub>C</sub> 178.5 (C=O), 159.6 (C=ONH), 156.3 (d, *J*<sub>C-F</sub> = 250.7 Hz, C-F), 154.8 (Cq), 143.9 (Cq), 138.1 (Cq), 135.4 (C=N), 131.4 (Cq), 130.6 (ArCH), 129.3 (ArCH), 128.3 (ArCH), 126.6 (Cq), 125.8 (d, *J* = 15.1 Hz, Cq), 125.6 (d, *J* = 4.4 Hz, ArCH), 122.2 (ArCH), 121.6 (ArCH), 115.8 (ArCH), 111.3 (ArCH), 77.7 (Cq-spiro), 60.5 (C(CH<sub>3</sub>)<sub>3</sub>), 54.6 (CH), 29.5 (C(CH<sub>3</sub>)<sub>3</sub>); LRMS *m/z* (ESI<sup>+</sup>) [Found: 541, C<sub>27</sub>H<sub>23</sub>Cl<sub>2</sub>FN<sub>4</sub>O<sub>3</sub> requires [M+H]<sup>+</sup> 541]; HPLC Method 1 (A): Retention time 7.2 min, 99.9%.

#### 4.1.4. General procedure for the synthesis of spiroprazoline oxindole amide derivatives (3b-h)

To a solution spiroprazoline oxindole **3a** (1.0 eq.) in a mixture of THF/MeOH/H<sub>2</sub>O (3:2:1) (0.09 mmol/mL) was added lithium hydroxide (10 eq.). The reaction mixture was stirred 30 min at room temperature and, after this time, neutralized with 1 M aqueous HCl and concentrated *in vacuo* to afford the correspondent carboxylic acid (R<sub>f</sub> 0.00 (5% MeOH in CH<sub>2</sub>Cl<sub>2</sub>)). The previous crude was dissolved in anhydrous DMF (6.8 mL/mmol of acid) and DIPEA, (2.0 eq.), HOBt (1.5 eq.) and TBTU (1.5 eq.) were added at room temperature. The reaction mixture was stirred at room temperature for 15 min. The appropriate amine (1.1 eq.) in DMF (4.6 mL/mmol amine) was added to the previous flask. The reaction mixture was stirred at room temperature for 18–21 h. After that time, the reaction mixture was diluted with H<sub>2</sub>O and extracted with EtOAc. The combined organic phases were washed with H<sub>2</sub>O, brine, dried over Na<sub>2</sub>SO<sub>4</sub>, filtered, and concentrated *in vacuo*. The crude residue was purified by silica gel flash chromatography to yield the title the

spiroprazoline oxindole amide derivative.

**6-Chloro-2'-(4-chlorophenyl)-4'-(3-hydroxyphenyl)-2-oxo-*N*-(3-(3-phenyl-1*H*-pyrazol-1-yl)phenyl)-2',4'-dihydrospiro [indoline-3,3'-pyrazole]-5'-carboxamide (3b):** To a solution of ethyl 6-chloro-2'-(4-chlorophenyl)-4'-(3-hydroxyphenyl)-2-oxo-2',4'-dihydrospiro [indoline-3,3'-pyrazole]-5'-carboxylate (**3a**) (30 mg, 0.060 mmol, 1.0 eq.) in a mixture of THF/MeOH/H<sub>2</sub>O (3:2:1) (0.7 mL) was added lithium hydroxide (15 mg, 0.60 mmol, 10 eq.). The reaction mixture was stirred 30 min at room temperature and, after this time, neutralized with 1 M aqueous HCl and concentrated *in vacuo* to afford the correspondent carboxylic acid (R<sub>f</sub> 0.00 (5% MeOH in CH<sub>2</sub>Cl<sub>2</sub>)). The previous crude was dissolved in anhydrous DMF (0.5 mL), followed by addition of DIPEA (21 μL, 0.121 mmol, 2.0 eq.), HOBt (13 mg, 0.090 mmol, 1.5 eq.) and TBTU (29 mg, 0.090 mmol, 1.5 eq.). The reaction mixture was stirred at room temperature for 15 min. 3-(3-Phenyl-1*H*-pyrazol-1-yl)aniline (17 mg, 0.066 mmol, 1.1 eq.) in DMF (0.3 mL) was added to the previous flask, and the reaction was stirred at room temperature for 18 h. The reaction mixture was diluted with H<sub>2</sub>O (10 mL) and extracted with EtOAc (3 × 5 mL). The combined organic phases were washed with H<sub>2</sub>O, brine, dried over Na<sub>2</sub>SO<sub>4</sub>, filtered, and concentrated *in vacuo*. The crude residue was purified by silica gel flash chromatography (elution with 5% MeOH in CH<sub>2</sub>Cl<sub>2</sub>) to yield the title compound as a yellow solid (18 mg, 0.026 mmol, 40%); R<sub>f</sub> 0.24 (5% MeOH in CH<sub>2</sub>Cl<sub>2</sub>); m.p.: 189–191 °C; <sup>1</sup>H NMR (300 MHz; CD<sub>3</sub>OD) δ<sub>H</sub> 8.26 (t, *J* = 2.1 Hz, 1H, ArH), 8.20 (d, *J* = 2.6 Hz, 1H, ArH), 7.98–7.84 (m, 2H, ArH), 7.66 (dd, *J* = 8.0, 2.1 Hz, 1H, ArH), 7.58 (dd, *J* = 8.0, 2.1 Hz, 1H, ArH), 7.51–7.28 (m, 4H, ArH), 7.18–7.12 (m, 2H, ArH), 7.06 (t, *J* = 7.8 Hz, 1H, ArH), 7.01–6.94 (m, 2H, ArH), 6.91 (d, *J* = 1.9 Hz, 1H, ArH), 6.87 (d, *J* = 2.6 Hz, 1H, ArH), 6.67–6.63 (m, 2H, ArH), 6.54–6.46 (m, 2H, ArH), 6.43 (d, *J* = 8.1 Hz, 1H, ArH), 5.11 (s, 1H); <sup>13</sup>C NMR (75 MHz; CD<sub>3</sub>OD) δ<sub>C</sub> 177.0 (C=O), 159.9 (C=ONH), 157.5 (Cq), 153.0 (Cq), 144.8 (Cq), 142.6 (Cq), 141.2 (Cq), 140.5 (Cq), 139.1 (Cq), 135.6 (Cq), 135.4 (C=N), 132.9 (Cq), 129.5 (ArCH), 129.4 (ArCH), 128.7 (ArCH), 128.5 (ArCH), 128.2 (ArCH), 127.7 (ArCH), 127.4 (Cq), 127.3 (ArCH), 125.5 (ArCH), 122.7 (Cq), 121.7 (ArCH), 119.3 (ArCH), 118.0 (ArCH), 117.1 (ArCH), 115.1 (ArCH), 114.9 (ArCH), 114.4 (ArCH), 110.8 (ArCH), 110.7 (ArCH), 104.8 (ArCH), 77.3 (Cq-spiro); LRMS *m/z* (ESI<sup>+</sup>) [Found: 685, C<sub>38</sub>H<sub>26</sub>Cl<sub>2</sub>N<sub>6</sub>O<sub>3</sub> requires [M+H]<sup>+</sup> 685]; HPLC Method 1 (B): Retention time 4.1 min, 99.8%.

**6-Chloro-2'-(4-chlorophenyl)-4'-(3-hydroxyphenyl)-*N*-(4-hydroxyphenyl)-2-oxo-2',4'-dihydrospiro [indoline-3,3'-pyrazole]-5'-carboxamide (3c):** To a solution of ethyl 6-chloro-2'-(4-chlorophenyl)-4'-(3-hydroxyphenyl)-2-oxo-2',4'-dihydrospiro [indoline-3,3'-pyrazole]-5'-carboxylate (**3a**) (30 mg, 0.060 mmol, 1.0 eq.) in a mixture of THF/MeOH/H<sub>2</sub>O (3:2:1) (0.7 mL) was added lithium hydroxide (15 mg, 0.60 mmol, 10 eq.). The reaction mixture was stirred 30 min at room temperature and, after this time, neutralized with 1 M aqueous HCl and concentrated *in vacuo* to afford the correspondent carboxylic acid (R<sub>f</sub> 0.00 (5% MeOH in CH<sub>2</sub>Cl<sub>2</sub>)). The previous crude was dissolved in anhydrous DMF (0.5 mL), followed by addition of DIPEA (21 μL, 0.121 mmol, 2.0 eq.), HOBt (13 mg, 0.090 mmol, 1.5 eq.) and TBTU (29 mg, 0.090 mmol, 1.5 eq.). The reaction mixture was stirred at room temperature for 15 min. 4-Aminophenol (8 mg, 0.066 mmol, 1.1 eq.) in DMF (0.3 mL) was added to the previous flask, and the reaction was stirred at room temperature for 19 h. The reaction mixture was diluted with H<sub>2</sub>O (10 mL) and extracted with EtOAc (3 × 5 mL). The combined organic phases were washed with H<sub>2</sub>O, brine, dried over Na<sub>2</sub>SO<sub>4</sub>, filtered, and concentrated *in vacuo*. The crude residue was purified by silica gel flash chromatography (elution with 5% MeOH in CH<sub>2</sub>Cl<sub>2</sub>) to yield the title compound as a yellow solid (22 mg, 0.039 mmol, 65%); R<sub>f</sub> 0.38 (10% MeOH in CH<sub>2</sub>Cl<sub>2</sub>); m.p.: 218–219 °C; <sup>1</sup>H NMR (300 MHz; (CD<sub>3</sub>)<sub>2</sub>CO) δ<sub>H</sub> 9.61 (br s, 1H, OH), 8.28 (br s, 1H, NH), 7.65–7.54 (m, 2H, ArH), 7.23–7.13 (m, 2H, ArH), 7.05 (t, *J* = 8.1 Hz, 1H, ArH), 6.98 (d, *J* = 1.9 Hz, 1H, ArH), 6.97–6.91 (m, 2H, ArH), 6.85–6.77 (m, 2H, ArH), 6.70–6.65 (m, 2H, ArH), 6.61–6.52 (m, 2H, ArH), 6.47 (d, *J* = 8.1 Hz, 1H, ArH), 5.11 (s, 1H, CH); <sup>13</sup>C NMR (75 MHz; (CD<sub>3</sub>)<sub>2</sub>CO) δ<sub>C</sub> 176.6

(C=O), 159.1 (C=ONH), 158.5 (Cq), 154.8 (Cq), 147.1 (Cq), 143.9 (Cq), 142.7 (Cq), 136.8 (C=N), 135.9 (Cq), 131.6 (Cq), 130.4 (ArCH), 129.7 (ArCH), 128.3 (ArCH), 127.3 (Cq), 123.8 (Cq), 122.5 (ArCH), 122.4 (ArCH), 120.5 (ArCH), 117.9 (ArCH), 116.4 (ArCH), 116.0 (ArCH), 115.8 (ArCH), 111.7 (ArCH), 77.6 (Cq-spiro), 61.9 (C=H); LRMS m/z (ESI<sup>+</sup>) [Found: 559, C<sub>29</sub>H<sub>20</sub>Cl<sub>2</sub>N<sub>4</sub>O<sub>4</sub> requires [M+H]<sup>+</sup> 559]; HPLC Method 1 (A): Retention time 4.6 min, 99.5%.

**6-Chloro-2'-(4-chlorophenyl)-N-(4-hydroxyphenethyl)-4'-(3-hydroxyphenyl)-2-oxo-2',4'-dihydrospiro [indoline-3,3'-pyrazole]-5'-carboxamide (3d):** To a solution of ethyl 6-chloro-2'-(4-chlorophenyl)-4'-(3-hydroxyphenyl)-2-oxo-2',4'-dihydrospiro [indoline-3,3'-pyrazole]-5'-carboxylate (**3a**) (20 mg, 0.040 mmol, 1.0 eq.) in a mixture of THF/MeOH/H<sub>2</sub>O (3:2:1) (0.5 mL) was added lithium hydroxide (22 mg, 0.40 mmol, 10 eq.). The reaction mixture was stirred 30 min at room temperature and, after this time, neutralized with 1 M aqueous HCl and concentrated *in vacuo* to afford the correspondent carboxylic acid (R<sub>f</sub> 0.00 (5% MeOH in CH<sub>2</sub>Cl<sub>2</sub>)). The previous crude was dissolved in anhydrous DMF (0.3 mL), followed by addition of DIPEA (14 μL, 0.080 mmol, 2.0 eq.), HOBt (9 mg, 0.060 mmol, 1.5 eq.) and TBTU (20 mg, 0.060 mmol, 1.5 eq.). The reaction mixture was stirred at room temperature for 15 min. 4-(2-Aminoethyl)phenol (6 mg, 0.044 mmol, 1.1 eq.) in DMF (0.2 mL) was added to the previous flask, and the reaction was stirred at room temperature for 18 h. The reaction mixture was diluted with H<sub>2</sub>O (5 mL) and extracted with EtOAc (3 × 2 mL). The combined organic phases were washed with H<sub>2</sub>O, brine, dried over Na<sub>2</sub>SO<sub>4</sub>, filtered, and concentrated *in vacuo*. The crude residue was purified by silica gel flash chromatography (elution with 5% MeOH in CH<sub>2</sub>Cl<sub>2</sub>) to yield the title compound as an orange foam (12 mg, 0.021 mmol, 52%); R<sub>f</sub> 0.34 (10% MeOH in CH<sub>2</sub>Cl<sub>2</sub>); m.p.: 181–183 °C; <sup>1</sup>H NMR (300 MHz; CD<sub>3</sub>OD) δ<sub>H</sub> 7.14–7.08 (m, 2H, ArH), 7.08–6.99 (m, 3H, ArH), 6.89 (d, J = 1.9 Hz, 1H, ArH), 6.86–6.79 (m, 2H, ArH), 6.76–6.68 (m, 2H, ArH), 6.67–6.60 (m, 2H, ArH), 6.41–6.35 (m, 3H, ArH), 4.99 (s, 1H, CH), 3.55–3.39 (m, 2H, CH<sub>2</sub>CH<sub>2</sub>PhOH), 2.76 (t, J = 7.3 Hz, 2H, CH<sub>2</sub>CH<sub>2</sub>PhOH); <sup>13</sup>C NMR (75 MHz; CD<sub>3</sub>OD) δ<sub>C</sub> 178.5 (C=O), 163.0 (C=ONH), 158.9 (Cq), 156.9 (Cq), 146.4 (Cq), 143.9 (Cq), 142.9 (Cq), 136.9 (Cq), 136.7 (C=N), 131.1 (Cq), 130.8 (ArCH), 130.8 (ArCH), 129.9 (ArCH), 128.6 (ArCH), 128.4 (Cq), 124.2 (Cq), 123.1 (ArCH), 120.7 (ArCH), 118.2 (ArCH), 116.5 (ArCH), 116.3 (ArCH), 116.2 (ArCH), 112.1 (ArCH), 78.5 (Cq-spiro), 62.4 (CH), 42.4 (CH<sub>2</sub>CH<sub>2</sub>PhOH), 35.7 (CH<sub>2</sub>CH<sub>2</sub>PhOH); LRMS m/z (ESI<sup>+</sup>) [Found: 587, C<sub>31</sub>H<sub>24</sub>Cl<sub>2</sub>N<sub>4</sub>O<sub>4</sub> requires [M+H]<sup>+</sup> 587]; HPLC Method 1 (A): Retention time 7.2 min, 99.9%.

**6-Chloro-2'-(4-chlorophenyl)-N-((1-hydroxycyclobutyl)methyl)-4'-(3-hydroxyphenyl)-2-oxo-2',4'-dihydrospiro [indoline-3,3'-pyrazole]-5'-carboxamide (3e):** To a solution of ethyl 6-chloro-2'-(4-chlorophenyl)-4'-(3-hydroxyphenyl)-2-oxo-2',4'-dihydrospiro [indoline-3,3'-pyrazole]-5'-carboxylate (**3a**) (30 mg, 0.060 mmol, 1.0 eq.) in a mixture of THF/MeOH/H<sub>2</sub>O (3:2:1) (0.7 mL) was added lithium hydroxide (15 mg, 0.60 mmol, 10 eq.). The reaction mixture was stirred 30 min at room temperature and, after this time, neutralized with 1 M aqueous HCl and concentrated *in vacuo* to afford the correspondent carboxylic acid (R<sub>f</sub> 0.00 (5% MeOH in CH<sub>2</sub>Cl<sub>2</sub>)). The previous crude was dissolved in anhydrous DMF (0.5 mL), followed by addition of DIPEA (21 μL, 0.121 mmol, 2.0 eq.), HOBt (13 mg, 0.090 mmol, 1.5 eq.) and TBTU (29 mg, 0.090 mmol, 1.5 eq.). The reaction mixture was stirred at room temperature for 15 min. 1-(Aminomethyl)cyclobutan-1-ol (11 μL, 0.066 mmol, 1.1 eq.) in DMF (0.3 mL) was added to the previous flask, and the reaction was stirred at room temperature for 21 h. The reaction mixture was diluted with H<sub>2</sub>O (10 mL) and extracted with EtOAc (3 × 5 mL). The combined organic phases were washed with H<sub>2</sub>O, brine, dried over Na<sub>2</sub>SO<sub>4</sub>, filtered, and concentrated *in vacuo*. The crude residue was purified by silica gel flash chromatography (elution with 5% MeOH in CH<sub>2</sub>Cl<sub>2</sub>) to yield the title compound as a pale-yellow foam (14 mg, 0.025 mmol, 42%); R<sub>f</sub> 0.22 (5% MeOH in CH<sub>2</sub>Cl<sub>2</sub>); m.p.: 183–185 °C; <sup>1</sup>H NMR (300 MHz; (CD<sub>3</sub>)<sub>2</sub>CO) δ<sub>H</sub> 9.95 (br s, 1H, OH-phenol), 8.32 (br s, 1H, NH), 7.82 (t, J = 6.0 Hz, 1H, NH-amide), 7.21–7.09 (m, 2H, ArH), 7.04 (t, J =

8.1 Hz, 1H, ArH), 6.97 (d, J = 1.9 Hz, 1H, ArH), 6.92–6.83 (m, 2H, ArH), 6.72–6.60 (m, 2H, ArH), 6.55–6.46 (m, 2H, ArH), 6.45 (d, J = 8.1 Hz, 1H, ArH), 5.06 (s, 1H, CH), 4.55 (br s, 1H, OH), 3.49 (t, J = 5.5 Hz, 2H, NHCH<sub>2</sub>), 2.08–1.97 (m, 4H, CH<sub>2</sub>CH<sub>2</sub>CH<sub>2</sub>), 1.73–1.60 (m, 1H, CH<sub>2</sub>CH<sub>2</sub>CH<sub>2</sub>), 1.56–1.46 (m, 1H, CH<sub>2</sub>CH<sub>2</sub>CH<sub>2</sub>); <sup>13</sup>C NMR (75 MHz; (CD<sub>3</sub>)<sub>2</sub>CO) δ<sub>C</sub> 176.7 (C=O), 162.2 (C=ONH), 158.5 (Cq), 146.7 (Cq), 143.9 (Cq), 142.8 (Cq), 136.9 (C=N), 135.9 (Cq), 130.3 (ArCH), 129.7 (ArCH), 128.3 (ArCH), 127.3 (Cq), 123.9 (Cq), 122.4 (ArCH), 120.5 (ArCH), 117.8 (ArCH), 116.4 (ArCH), 115.8 (ArCH), 111.7 (ArCH), 77.5 (Cq-spiro), 75.0 (Cq-OH), 62.0 (CH), 47.3 (NHCH<sub>2</sub>), 34.8 (CH<sub>2</sub>CH<sub>2</sub>CH<sub>2</sub>), 34.7 (CH<sub>2</sub>CH<sub>2</sub>CH<sub>2</sub>), 12.3 (CH<sub>2</sub>CH<sub>2</sub>CH<sub>2</sub>); LRMS m/z (ESI<sup>+</sup>) [Found: 551, C<sub>28</sub>H<sub>24</sub>Cl<sub>2</sub>N<sub>4</sub>O<sub>4</sub> requires [M+Na]<sup>+</sup> 551]; HPLC Method 1 (C): Retention time 4.2 min, 97.5%.

**N-(3-(1H-pyrazol-1-yl)phenyl)-6-chloro-2'-(4-chlorophenyl)-4'-(3-hydroxyphenyl)-2-oxo-2',4'-dihydrospiro [indoline-3,3'-pyrazole]-5'-carboxamide (3f):** To a solution of ethyl 6-chloro-2'-(4-chlorophenyl)-4'-(3-hydroxyphenyl)-2-oxo-2',4'-dihydrospiro [indoline-3,3'-pyrazole]-5'-carboxylate (**3a**) (30 mg, 0.060 mmol, 1.0 eq.) in a mixture of THF/MeOH/H<sub>2</sub>O (3:2:1) (0.7 mL) was added lithium hydroxide (15 mg, 0.60 mmol, 10 eq.). The reaction mixture was stirred 30 min at room temperature and, after this time, neutralized with 1 M aqueous HCl and concentrated *in vacuo* to afford the correspondent carboxylic acid (R<sub>f</sub> 0.00 (5% MeOH in CH<sub>2</sub>Cl<sub>2</sub>)). The previous crude was dissolved in anhydrous DMF (0.5 mL), followed by addition of DIPEA (21 μL, 0.121 mmol, 2.0 eq.), HOBt (13 mg, 0.090 mmol, 1.5 eq.) and TBTU (29 mg, 0.090 mmol, 1.5 eq.). The reaction mixture was stirred at room temperature for 15 min. 3-(1H-Pyrazol-1-yl)aniline (12 μL, 0.066 mmol, 1.1 eq.) in DMF (0.3 mL) was added to the previous flask, and the reaction was stirred at room temperature for 20 h. The reaction mixture was diluted with H<sub>2</sub>O (10 mL) and extracted with EtOAc (3 × 5 mL). The combined organic phases were washed with H<sub>2</sub>O, brine, dried over Na<sub>2</sub>SO<sub>4</sub>, filtered, and concentrated *in vacuo*. The crude residue was purified by silica gel flash chromatography (elution with 5% MeOH in CH<sub>2</sub>Cl<sub>2</sub>) to yield the title compound as a yellow solid (18 mg, 0.029 mmol, 46%); R<sub>f</sub> 0.26 (5% MeOH in CH<sub>2</sub>Cl<sub>2</sub>); m.p.: 232–233 °C; <sup>1</sup>H NMR (300 MHz; (CD<sub>3</sub>)<sub>2</sub>CO) δ<sub>H</sub> 9.97 (s, 1H, OH), 8.35 (t, 1H, J = 1.89 Hz, 1H, ArH), 8.31 (br s, 1H, NH), 8.26 (d, J = 2.5 Hz, 1H, ArH), 7.75 (d, J = 8.1 Hz, 1H, ArH), 7.68 (d, J = 1.5 Hz, 1H, ArH), 7.56 (d, J = 9.0 Hz, 1H, ArH), 7.43 (t, J = 8.1 Hz, 1H, ArH), 7.23–7.12 (m, 2H, ArH), 7.06 (t, J = 8.1 Hz, 1H, ArH), 7.03–6.94 (m, 3H, ArH), 6.72–6.65 (m, 2H, ArH), 6.62–6.52 (m, 2H, ArH), 6.52–6.42 (m, 2H, ArH), 5.15 (s, 1H, CH); <sup>13</sup>C NMR (75 MHz; (CD<sub>3</sub>)<sub>2</sub>CO) δ<sub>C</sub> 176.5 (C=O), 159.8 (C=ONH), 158.5 (Cq), 146.4 (Cq), 143.9 (Cq), 142.5 (Cq), 141.6 (Cq), 141.6 (ArCH), 140.7 (Cq), 140.7 (ArCH), 136.8 (Cq), 136.1 (C=N), 130.6 (ArCH), 130.5 (ArCH), 129.9 (ArCH), 129.7 (ArCH), 128.4 (ArCH), 127.8 (ArCH), 127.6 (Cq), 123.7 (Cq), 122.5 (ArCH), 120.5 (ArCH), 118.1 (ArCH), 116.4 (ArCH), 115.9 (ArCH), 114.6 (ArCH), 111.8 (ArCH), 111.0 (ArCH), 108.4 (ArCH), 77.8 (Cq-spiro), 61.7 (CH); LRMS m/z (ESI<sup>+</sup>) [Found: 609, C<sub>32</sub>H<sub>22</sub>Cl<sub>2</sub>N<sub>6</sub>O<sub>3</sub> requires [M+H]<sup>+</sup> 609]; HPLC Method 1 (C): Retention time 7.3 min, 98.6%.

**6-Chloro-2'-(4-chlorophenyl)-N-(2-hydroxyethyl)-4'-(3-hydroxyphenyl)-2-oxo-2',4'-dihydrospiro [indoline-3,3'-pyrazole]-5'-carboxamide (3g):** To a solution of ethyl 6-chloro-2'-(4-chlorophenyl)-4'-(3-hydroxyphenyl)-2-oxo-2',4'-dihydrospiro [indoline-3,3'-pyrazole]-5'-carboxylate (**3a**) (20 mg, 0.040 mmol, 1.0 eq.) in a mixture of THF/MeOH/H<sub>2</sub>O (3:2:1) (0.5 mL) was added lithium hydroxide (22 mg, 0.40 mmol, 10 eq.). The reaction mixture was stirred 30 min at room temperature and, after this time, neutralized with 1 M aqueous HCl and concentrated *in vacuo* to afford the correspondent carboxylic acid (R<sub>f</sub> 0.00 (5% MeOH in CH<sub>2</sub>Cl<sub>2</sub>)). The previous crude was dissolved in anhydrous DMF (0.3 mL), followed by the addition of DIPEA (14 μL, 0.080 mmol, 2.0 eq.), HOBt (9 mg, 0.060 mmol, 1.5 eq.) and TBTU (20 mg, 0.060 mmol, 1.5 eq.). The reaction mixture was stirred at room temperature for 15 min. 2-Aminoethan-1-ol (3 μL, 0.044 mmol, 1.1 eq.) in DMF (0.20 mL) was added to the previous flask, and the reaction was stirred at room temperature for 18 h. The reaction mixture was diluted

with H<sub>2</sub>O (5 mL) and extracted with EtOAc (3 × 2 mL). The combined organic phases were washed with H<sub>2</sub>O, brine, dried over Na<sub>2</sub>SO<sub>4</sub>, filtered, and concentrated *in vacuo*. The crude residue was purified by silica gel flash chromatography (elution with 5% MeOH in CH<sub>2</sub>Cl<sub>2</sub>) to yield the title compound as a yellow foam (15 mg, 0.029 mmol, 70%); R<sub>f</sub> 0.28 (10% MeOH in CH<sub>2</sub>Cl<sub>2</sub>); m.p.: 202–203 °C; <sup>1</sup>H NMR (500 MHz; CD<sub>3</sub>OD) δ<sub>H</sub> 7.16–7.10 (m, 2H, ArH), 7.03 (t, *J* = 7.8 Hz, 1H, ArH), 6.89 (d, *J* = 1.9 Hz, 1H, ArH), 6.88–6.84 (m, 2H, ArH), 6.63 (dt, *J* = 8.4, 2.4 Hz, 2H, ArH), 6.42 (d, *J* = 7.8 Hz, 1H, ArH), 6.40–6.35 (m, 2H, ArH), 4.99 (s, 1H, CH), 3.67 (t, *J* = 6.1 Hz, 2H, CH<sub>2</sub>CH<sub>2</sub>OH), 3.54–3.36 (m, 2H, CH<sub>2</sub>CH<sub>2</sub>OH); <sup>13</sup>C NMR (126 MHz; CD<sub>3</sub>OD) δ<sub>C</sub> 178.5 (C=O), 163.3 (C=ONH), 158.9 (Cq), 146.2 (Cq), 144.0 (Cq), 142.8 (Cq), 136.9 (Cq), 136.8 (C=N), 130.7 (ArCH), 129.9 (ArCH), 128.6 (ArCH), 128.5 (Cq), 124.2 (Cq), 123.1 (ArCH), 120.7 (ArCH), 118.2 (ArCH), 116.4 (ArCH), 116.2 (ArCH), 112.1 (ArCH), 78.5 (Cq-spiro), 62.4 (CH), 61.5 (CH<sub>2</sub>CH<sub>2</sub>OH), 42.9 (CH<sub>2</sub>CH<sub>2</sub>OH); LRMS *m/z* (ESI<sup>+</sup>) [Found: 511, C<sub>25</sub>H<sub>20</sub>Cl<sub>2</sub>N<sub>4</sub>O<sub>4</sub> requires [M+H]<sup>+</sup> 511]; HPLC Method 1 (A): Retention time 6.2 min, 99.6%.

**6-Chloro-2'-(4-chlorophenyl)-4'-(3-hydroxyphenyl)-N-(2-(methylamino)ethyl)-2-oxo-2',4'-dihydrospiro[indoline-3,3'-pyrazole]-5'-carboxamide (3h):** To a solution of ethyl 6-chloro-2'-(4-chlorophenyl)-4'-(3-hydroxyphenyl)-2-oxo-2',4'-dihydrospiro [indoline-3,3'-pyrazole]-5'-carboxylate (**3a**) (30 mg, 0.060 mmol, 1.0 eq.) in a mixture of THF/MeOH/H<sub>2</sub>O (3:2:1) (0.7 mL) was added lithium hydroxide (15 mg, 0.60 mmol, 10 eq.). The reaction mixture was stirred 30 min at room temperature and, after this time, neutralized with 1 M aqueous HCl and concentrated *in vacuo* to afford the correspondent carboxylic acid (R<sub>f</sub> 0.00 (5% MeOH in CH<sub>2</sub>Cl<sub>2</sub>)). The previous crude was dissolved in anhydrous DMF (0.5 mL), followed by addition of DIPEA (21 μL, 0.121 mmol, 2.0 eq.), HOBt (13 mg, 0.090 mmol, 1.5 eq.) and TBTU (29 mg, 0.090 mmol, 1.5 eq.). The reaction mixture was stirred at room temperature for 15 min *tert*-Butyl (2-aminoethyl)(methyl)carbamate (13 mg, 0.066 mmol, 1.1 eq.) in DMF (0.3 mL) was added to the previous flask, and the reaction was stirred at room temperature for 18 h. The reaction mixture was diluted with H<sub>2</sub>O (10 mL) and extracted with EtOAc (3 × 5 mL). The combined organic phases were washed with H<sub>2</sub>O, brine, dried over Na<sub>2</sub>SO<sub>4</sub>, filtered, and concentrated *in vacuo*. The crude residue was purified by silica gel flash chromatography (elution with 5% MeOH in CH<sub>2</sub>Cl<sub>2</sub>) to yield *tert*-butyl (2-(6-chloro-2'-(4-chlorophenyl)-4'-(3-hydroxyphenyl)-2-oxo-2',4'-dihydrospiro[indoline-3,3'-pyrazole]-5'-carboxamido)ethyl)(methyl)carbamate as a pale-yellow oil (21 mg, 0.033 mmol, 55%); R<sub>f</sub> 0.27 (5% MeOH in CH<sub>2</sub>Cl<sub>2</sub>); LRMS *m/z* (ESI<sup>+</sup>) [Found: 622, C<sub>31</sub>H<sub>31</sub>Cl<sub>2</sub>N<sub>5</sub>O<sub>5</sub> requires [M - H]<sup>-</sup> 622].

To a solution of *tert*-butyl (2-(6-chloro-2'-(4-chlorophenyl)-4'-(3-hydroxyphenyl)-2-oxo-2',4'-dihydrospiro[indoline-3,3'-pyrazole]-5'-carboxamido)ethyl)(methyl)carbamate (20 mg, 0.032 mmol, 1.0 eq.) in CH<sub>2</sub>Cl<sub>2</sub> (0.25 mL) was added trifluoroacetic acid (36 μL, 0.036 mmol, 15 eq.), and the reaction mixture was stirred at room temperature for 1 h. After that time, the reaction mixture was concentrated *in vacuo* and the crude oil was dissolved in CH<sub>2</sub>Cl<sub>2</sub> (1 mL) and DIPEA (6 μL, 0.033 mmol, 1.0 eq.) was added. The solution was stirred 1 h at room temperature and, then, concentrated *in vacuo*. The resulted crude oil was purified by a short silica gel flash chromatography (elution with 5%–10% MeOH in CH<sub>2</sub>Cl<sub>2</sub>) to yield the title compound as a pale-yellow foam (15 mg, 0.029 mmol, 89%); R<sub>f</sub> 0.16 (15% MeOH in CH<sub>2</sub>Cl<sub>2</sub>); m.p.: 212–214 °C; <sup>1</sup>H NMR (300 MHz; CD<sub>3</sub>CD) δ<sub>H</sub> 7.12 (d, *J* = 8.9 Hz, 2H, ArH), 7.04 (t, *J* = 7.9 Hz, 1H, ArH), 6.95–6.77 (m, 3H, ArH), 6.64 (dd, *J* = 8.1, 1.9 Hz, 2H, ArH), 6.48–6.27 (m, 3H, ArH), 4.98 (s, 1H, CH), 3.69–3.39 (m, 2H, CH<sub>2</sub>CH<sub>2</sub>NHCH<sub>3</sub>), 2.96 (t, *J* = 6.1 Hz, 2H, CH<sub>2</sub>CH<sub>2</sub>NHCH<sub>3</sub>), 2.55 (s, 3H, CH<sub>3</sub>); <sup>13</sup>C NMR (75 MHz; CD<sub>3</sub>CD) δ<sub>C</sub> 178.5 (C=O), 163.7 (C=ONH), 158.9 (Cq), 145.9 (Cq), 144.0 (Cq), 142.7 (Cq), 137.0 (Cq), 136.7 (C=N), 130.8 (ArCH), 129.9 (ArCH), 128.6 (Cq), 128.6 (ArCH), 124.0 (Cq), 123.1 (ArCH), 120.7 (ArCH), 118.3 (ArCH), 116.5 (ArCH), 116.2 (ArCH), 112.2 (ArCH), 78.5 (Cq-spiro), 62.2 (CH), 50.9 (CH<sub>2</sub>CH<sub>2</sub>NHCH<sub>3</sub>), 38.3 (CH<sub>2</sub>CH<sub>2</sub>NHCH<sub>3</sub>), 34.8 (CH<sub>3</sub>); LRMS *m/z* (ESI<sup>+</sup>) [Found: 524, C<sub>26</sub>H<sub>23</sub>Cl<sub>2</sub>N<sub>5</sub>O<sub>3</sub> requires [M+H]<sup>+</sup> 524]; HPLC Method 1

(D): Retention time 7.8 min, 97.0%.

## 4.2. Biological studies

### 4.2.1. Cell lines and culture

Human colorectal cancer cell line HCT116 (ATCC® CCL-247™), human osteosarcoma cancer cell line SJSA-1 (CRL- ATCC® 2098™), human prostate adenocarcinoma cancer cell line LNCaP (ATCC® CRL-1740™), human breast adenocarcinoma cancer cell line MCF-7 (ATCC® HTB-22™), and human embryonic kidney epithelial cell line HEK 293T (ATCC® CRL-11268™) were obtained from the American Type Culture Collection (ATCC®). Human colorectal cancer cell line HCT116 p53<sup>(-/-)</sup> was obtained from the GRCF Cell Center and Biorepository (Johns Hopkins University, School of Medicine, Baltimore, MD, USA). Cells were grown in McCoy's 5A (HCT116), RPMI 1640 (LNCaP and HEK293T) and DMEM (MCF-7), all supplemented with 10% fetal bovine serum (FBS). Additionally, HCT116, LNCaP, and HEK293T cell media were supplemented with 1% antibiotic/antimycotic solution, while MCF-7 cell media was supplemented with 1% GlutaMAX™ and 1% penicillin/streptomycin solution. All cell media and supplements were acquired from Gibco, ThermoFisher. Human glioblastoma (U87MG) and human neuroblastoma (SHSY-5Y) cell lines were obtained from the National Institute for Cancer Research of Genova (Italy). The U87 and SHSY-5Y cells were grown in RPMI and DMEM F-12 medium, respectively, supplemented with 10% FBS, 2 mM l-glutamine, 100 U/mL penicillin, 100 mg/mL streptomycin and 1% non-essential amino acids. All cell lines were maintained at 37 °C in a humidified atmosphere of 5% CO<sub>2</sub>. The human cells were seeded in tissue culture dishes (Sarstedt) and, once reached 80% confluence, were detached from the plate and treated as described in section 4.2.6.

### 4.2.2. In vitro antiproliferative assays

Cells were seeded at 1 × 10<sup>4</sup> cells/well (HCT116), 3 × 10<sup>3</sup> cells/well (SJSA-1, LNCaP and HEK293T) and 5 × 10<sup>3</sup> cells/well (MCF-7). The day before the experiments, cells were seeded in 96-well tissue culture plates and incubated with vehicle or compounds approximately 24 h after plating. Stock solutions of compounds were prepared in dimethyl sulfoxide (DMSO) and then, serially diluted in the culture medium and added to the cells. The final concentration of DMSO in culture medium, during the treatment, did not exceed 0.1% (v/v). All experiments were performed in parallel with DMSO vehicle control and nutlin-3a as positive control. Each compound's concentration and DMSO were tested in duplicate in a single experiment which was repeated at least three times. For IC<sub>50</sub> determination, the range of concentrations used was 1–100 μM with at least ten points concentrations. Cell viability was assessed 48 h (HCT116), 72 h (MCF7) or 96 h (SJSA-1, LNCaP and HEK293T) after compounds' incubation. The determination of cell viability was carried out by using (3-(4,5-dimethylthiazol-2-yl)-5-(3-carboxymethoxyphenyl)-2-(4-sulfophenyl)-2H-tetrazolium) (MTS) method. After the incubation time, cell media was removed and replaced with fresh medium containing MTS dye at 0.5 mg/mL. After 15–30 min of incubation, the absorbance was measured at 490 nm using GloMax® Multi Detection System (Sunnyvale, CA, USA).

### 4.2.3. Cell cycle analysis

Cell cycle analysis was performed using a standard propidium iodide (PI) staining procedure followed by flow cytometry analysis. SJSA-1 cells were seeded in tissue-culture dishes (35 mm) at 1 × 10<sup>5</sup> cells/dish and incubated with vehicle control or compound approximately 24 h after plating. After 96 h, cells were treated with TrypLE™ reagent, collected, and centrifuged at 800 g for 5 min, at 4 °C. The supernatant was discarded, cell pellets were resuspended in cold PBS and, an equal volume of 80% ice-cold ethanol (–20 °C) was added dropwise, while gently vortexing the cells. Samples were stored at –4 °C until data acquisition. For cell cycle analysis, cells were centrifuged again at 850 g for 5 min, at 4 °C, and cell pellets were resuspended in 25 μg/mL PI



(Fluka, Sigma-Aldrich) and 50 µg/mL RNase A (Sigma-Aldrich) in PBS and incubated for 30 min at 37 °C. Sample acquisition was performed using the Guava® easyCyte™ Flow Cytometer (Luminex, Texas, USA) with the acquisition of at least 10,000 events per sample<sup>23</sup>, and data analysis was carried out with Mod Fit LT™ 4.1 software (Verity Software House, Maine, USA).

#### 4.2.4. Evaluation of cell death

Cell death was evaluated by measurement of lactate dehydrogenase (LDH) release using the Cytotoxicity Detection Kit (LDH)<sup>PLUS</sup> (Roche Diagnostics GmbH, Mannheim, Germany), according to the manufacturer's instructions. After treatment of SJSA-1 cells with vehicle control (DMSO) or compound, supernatant (50 µL) was transferred into a 96-well plate and then incubated with 50 µL of assay substrate for 10–30 min, at room temperature, protected from light. Absorbance readings were measured at 490 nm, with 620 nm reference wavelength, using a Bio-Rad Model 680 microplate reader.

#### 4.2.5. Evaluation of apoptosis by flow cytometry

Evaluation of apoptosis by Flow Cytometry was performed using Annexin V-PE and 7-Aminoactinomycin D (7-AAD) double staining (Nexin assay, Luminex). This procedure discriminates cells that are viable, in early-stage apoptosis and in late-stage apoptosis. SJSA-1 cells were seeded in 24-well plates at  $1.8 \times 10^4$  cells/dish. On the day after, cells were treated with vehicle control (DMSO) or compounds for an additional time of 96 h. After, the supernatant was collected and cells were detached with Accutase, and then centrifuged at 500 g for 5 min at 4 °C. The cell pellet was resuspended in PBS containing 2% of FBS. Subsequently, 100 µL of cell suspension were mixed with 100 µL of Guava Nexin reagent and incubated for 20 min, at room temperature in the absence of light. Sample acquisition and data analysis of at least 5000 events per sample were performed using the Guava® easyCyte™ Flow Cytometer (Luminex) and Nexin software module.

#### 4.2.6. MDM2/p53 and MDM4/p53 complexes dissociation studies

A quantitative immunoenzymatic assay was performed on cell lysates obtained from U87MG cells (for p53/MDM2) or SHSY-5Y cells (for p53/MDM4) to evaluate the ability of compounds **1**, **2a**, **2q**, **3c**, **3f** and **3q** to dissociate the MDM2/p53 and MDM4/p53 complexes [21–24]. Briefly, the full-length anti-MDM2 (sc-965, Santa Cruz Biotechnologies) or anti-MDM4 (sc-74468, Santa Cruz Biotechnologies) was added into the wells of a 96-well micro test plate (Sarstedt) and incubated overnight at room temperature. U87MG or SHSY-5Y cells were suspended in lysis buffer (20 mM Tris HCl, 137 mM NaCl, 10% glycerol, 1% NONIDET40, 2 mM EDTA, pH 8) containing 1% of the protease inhibitor cocktail (SigmaAldrich), treated with different concentrations of compounds for 10 min at 25 °C under continuous shaking and then transferred to the precoated wells and incubated for 1 h 30 min. Then, 1% BSA was incubated in each well to block nonspecific sites for 30 min. Thereafter, the wells were washed and an anti-p53 antibody (70R-31561, Fitzgerald) was added and incubated for 2 h. Finally, after extensive washes, the wells were incubated with an anti-rabbit HRP conjugated antibody. The TMB substrate kit (Thermo Fisher Scientific) was employed to allow the colorimetric quantification of the complexes. Absorbance was measured at 450 nm.

#### 4.2.7. Data analysis

All data are expressed as mean ± standard deviation (SD) of at least three independent experiments. All statistical analysis was carried out using GraphPad Prism version 8.4.2 software (La Jolla, California, USA). Dose-response curves were built and IC<sub>50</sub> values determined using the log-(inhibitor) versus response – variable slope (four parameters) function. Normality of data values was determined by Shapiro-Wilk test. Differences between two groups were determined with Unpaired *t*-test or Mann-Whitney *U* test. Differences between three or more groups were assessed using Ordinary one-way ANOVA or Kruskal-Wallis test,

followed by Bonferroni or Dunn's multiple comparisons test, respectively. A *p*-value inferior to 0.05 was considered significant.

### 4.3. Computational methods

#### 4.3.1. Molecular docking

The binding poses and binding energies of the studied compounds were predicted by molecular docking simulations. The crystallographic structures of MDM2 and MDM4 were downloaded from the Protein Data Bank (PDB ID 4WT2 [25], PDB ID 3LBJ [26], and PDB ID 6Q9S and 6Q9L [13]). These structures were chosen according to structural similarity to the human homolog proteins, sequence length, and resolution. Fred program (OpenEye Scientific Software Santa Fe) and SMINA were used to carry out the molecular docking simulations.

**First screening:** The receptor was prepared with the make\_receptor utility of OEDOCKING (v. 3.4.0.2), the binding site cavity was detected by molecular probe and its shape potential had an outer contour of 1514 Å<sup>3</sup> (4WT2) and 1490 Å<sup>3</sup> (3LBJ) balanced between solvent and the protein. The docking procedure was validated by re-docking simulations with the co-crystallized ligand and its ability to correctly predict the binding poses of these inhibitors was tested. Chemical structures of synthesized compounds were stored in SMILES format. These structures were transformed into 3D structures with the assigned stereochemistry using OMEGA (v. 3.1.2.2, OpenEye Scientific Software, Santa Fe, NM, <http://www.eyesopen.com/>) [27]. Their protonation states were assigned for pH 7.4 using QUACPAC (v. 2.0.2.2, OpenEye Scientific Software, Santa Fe, NM, <http://www.eyesopen.com/>) [28]. Ligand energy minimization was performed with SZYBKI (v. 1.11.0.2, OpenEye Scientific Software, Santa Fe, NM, <http://www.eyesopen.com/>) using the MMFF94S force field [29], while conformational analysis was performed with OMEGA 3.1.2.2 with all parameters at their default values and allowing the storage of 400 conformers of each molecule [27].

Molecular docking was performed with the FRED docking program (OEDOCKING 3.4.0.2, OpenEye Scientific Software, Santa Fe, NM, <http://www.eyesopen.com/>) [30], using the high docking accuracy settings. Five poses of each molecule were stored. The accuracy of these simulations was validated by redocking the co-crystallized ligands in the binding sites of MDM2 (4WT2) and MDM4 (3LBJ), using these parameters, and comparison of the docking results with the binding pose of the co-crystallized ligands.

**Second and third screenings:** The crystallographic PDB structure 6Q9S was imported to MOE to remove water molecules, ligands, or any extra co-crystallized molecules. Only chain A was retained and protonated using default parameters using the Protonate 3D module of MOE. The chemical structures of the synthesized compounds were minimized with the default force-field (adjusting hydrogen and lone pairs by default) using MOE 2019.01 with the ionization state assigned at pH 7.0. All the ligands and receptor were converted to PDBQT format using the appropriate python script available through the AutoDock MGLTools (1.5.6). The binding site of MDM4 structure was defined by a docking box including the whole internal cavity containing the co-crystallized ligand (dimensions XYZ of 18.75, 21, 21 Å). All these parameters and scoring functions/docking programs were tested to best reproduce the binding pose of the co-crystallized ligand. Compounds were docked toward the MDM4 receptor already prepared using the molecular docking program SMINA ([sourceforge.net/projects/sminka/](https://sourceforge.net/projects/sminka/); version of Feb 12, 2019) and the Vinardo scoring function which is an improvement on the original Vina scoring function that performed best to reproduce the experimental pose.

#### 4.3.2. Generation of spiropyrazoline oxindoles 3

Starting with compound **3a**, a database of novel derivatives was obtained using the “Add Group to Ligand” module of MOE 2019.01 by loading the 6Q9S MDM4 protein and defining the connection point to add fragments to the initial scaffold. The parameters to constrain the saved derivatives were defined to retain only non-reactive molecules,

maximum molecular weight (MW) of 700, and a topological polar surface area (TPSA) between 40 and 140. The selected linker point to add the fragments was the OH. These novel compounds were also docked with SMINA using the above conditions. Based on the results of this screening, a second screening was also performed in a similar way by generating a novel database of derivatives by adding fragments to the NH of the amide linker. All the results were ranked by their score and visually inspected for promising interactions using MOE [31] and PyMOL [32].

#### 4.3.3. MM-PBSA calculations

The 6Q9L structure was imported in MOE and manipulated as 6Q9S to be prepared for docking with box dimensions XYZ of 18.75, 15.75, 22.5 Å and centered on the co-crystallized ligand.

The 6Q9L and the 6Q9S crystallographic structures prepared and used in the molecular docking calculations were inserted in a dodecahedron simulation box with a 1 nm of minimum distance between the protein and the box edges to obtain two different systems. The systems were solvated, neutralized by the addition of NaCl ions as needed, and minimized through a steep descent technique using default values. A 50 ps NVT run with the protein restrained was performed to allow the solvent to adjust to the protein and for the pressure to stabilize. Following, a 500 ps NpT run with the protein unconstrained was performed for the pressure to adjust to the target 1 bar pressure. Finally, a 500 ns production run was produced with a data collection file containing the dynamics written every 50 ps. All simulations were performed at 303 K, 1 bar, and a 2 fs time-step. Nose-Hoover and Parrinello-Rahman algorithms were used for the temperature and pressure couplings with 0.2 and 5.0 ps for the temperature and pressure couplings, respectively. All bonds with hydrogen light atoms were constrained using lincs and a 1.0 nm cut-off was used for the van der Waals interactions and for the real space PME calculation. All molecular dynamics simulations were performed using GROMACS v2021.2.

The systems containing the ligands to be tested were obtained by superimposing the MDM4 structure with the one present in the molecular dynamics simulation box and the molecular docking predicted pose used as the starting point by just inserting the molecule in the solvated and neutralized system. A simple steepest descent minimization while keeping the protein constrained was enough to remove the waters that clashed with the ligand in most of the systems. In the cases where this was not sufficient, all water molecules at distances less than 3 Å were removed. A similar protocol and parameters for the MDM4-ligand systems were used after this minimization step. The SwissParam server was used to generate the topologies and parameters for all ligands [33].

All MM-PBSA calculations were performed through the *g\_mmpbsa* program using the GROMACS simulations obtained for each MDM4-ligand or MDM2-ligand complex [34].

#### Declaration of competing interest

The authors declare that they have no known competing financial interests or personal relationships that could have appeared to influence the work reported in this paper.

#### Data availability

no shared data

#### Acknowledgments

This work was supported by National Funds (FCT/MEC, Fundação para a Ciência e Tecnologia and Ministério da Educação e Ciência) through UIDB/04138/2020 (iMed.Ulisboa), project PTDC/QUI-QOR/29664/2017, fellowships SFRH/BD/117931/2016 (M. Espadinha), SFRH/BD/137544/2018 (E. A. Lopes) and PD/BD/135467/2017 (V. Marques), and the Portuguese Mass Spectrometry Network (LISBOA-01-

0145-FEDER-402-022125). The NMR spectrometers are part of the National NMR Network (PTNMR) and are partially supported by Infrastructure Project N° 022161 (co-financed by FEDER through COMPETE 2020, POCI and PORL and FCT through PIDDAC). MM wish to thank the OpenEye Free Academic Licensing Programme for providing a free academic licence for molecular modeling and cheminformatics software.

#### Appendix A. Supplementary data

Supplementary data to this article can be found online at <https://doi.org/10.1016/j.ejmech.2022.114637>.

#### References

- [1] H. Sung, J. Ferlay, R.L. Siegel, M. Laversanne, I. Soerjomataram, A. Jemal, F. Bray, Global cancer statistics 2020: GLOBOCAN estimates of incidence and mortality worldwide for 36 cancers in 185 countries, *CA Cancer J Clin* 71 (2021) 209–249, <https://doi.org/10.3322/caac.21660>.
- [2] L. Zhong, Y. Li, L. Xiong, W. Wang, M. Wu, T. Yuan, W. Yang, C. Tian, Z. Miao, T. Wang, S. Yang, Small molecules in targeted cancer therapy: advances, challenges, and future perspectives, *Signal Transduct. Targeted Ther.* 6 (2021) 201, <https://doi.org/10.1038/s41392-021-00572-w>.
- [3] J. Zawacka-Pankau, G. Selivanova, Pharmacological reactivation of p53 as a strategy to treat cancer, *J. Intern. Med.* 277 (2015) 248–259, <https://doi.org/10.1111/joim.12336>.
- [4] A. Aguilar, J. Lu, L. Liu, D. Du, D. Bernard, D. McEachern, S. Przybranowski, X. Li, R. Luo, B. Wen, D. Sun, H. Wang, J. Wen, G. Wang, Y. Zhai, M. Guo, D. Yang, S. Wang, Discovery of 4-((3'R,4'S,5'R)-6'-chloro-4'-(3-chloro-2-fluorophenyl)-1'-ethyl-2'-oxodispiro[cyclohexane-1,2'-pyrrolidine-3',3'-indoline]-5'-carboxamido)bicyclo[2.2.2]octane-1-carboxylic acid (AA-115/APG-115): a potent and orally active murine double minute 2 (MDM2) inhibitor in clinical development, *J. Med. Chem.* 60 (2017) 2819–2839, <https://doi.org/10.1021/acs.jmedchem.6b01665>.
- [5] M.S. Islam, H.M. Ghawas, F.F. El-Senduny, A.M. Al-Majid, Y.A.M.M. Elshair, F. A. Badria, A. Barakat, Synthesis of new thiazolo-pyrrolidine-(spirooxindole) tethered to 3-acetylindole as anticancer agents, *Bioorg. Chem.* 82 (2019) 423–430, <https://doi.org/10.1016/j.bioorg.2018.10.036>.
- [6] A. Barakat, M.S. Islam, H.M. Ghawas, A.M. Al-Majid, F.F. El-Senduny, F.A. Badria, Y.A.M.M. Elshair, H.A. Ghabbour, Design and synthesis of new substituted spirooxindoles as potential inhibitors of the MDM2–p53 interaction, *Bioorg. Chem.* 86 (2019) 598–608, <https://doi.org/10.1016/j.bioorg.2019.01.053>.
- [7] G. Lotfy, Y.M. Abdel Aziz, M.M. Said, E.S.H. El Ashry, E.S.H. El Tamany, M.M. Abu-Serie, M. Teleb, A. Dömling, A. Barakat, Molecular hybridization design and synthesis of novel spirooxindole-based MDM2 inhibitors endowed with BCL2 signaling attenuation; a step towards the next generation p53 activators, *Bioorg. Chem.* 117 (2021), 105427, <https://doi.org/10.1016/j.bioorg.2021.105427>.
- [8] Y.M.A. Aziz, G. Lotfy, M.M. Said, E.S.H. El Ashry, E.S.H. El Tamany, S.M. Soliman, M.M. Abu-Serie, M. Teleb, S. Yousuf, A. Dömling, L.R. Domingo, A. Barakat, Design, synthesis, chemical and biochemical insights into novel hybrid spirooxindole-based p53-MDM2 inhibitors with potential Bcl2 signaling attenuation, *Front. Chem.* 9 (2021), <https://doi.org/10.3389/fchem.2021.735236>.
- [9] S. Wang, F.-E. Chen, Small-molecule MDM2 inhibitors in clinical trials for cancer therapy, *Eur. J. Med. Chem.* 236 (2022), 114334, <https://doi.org/10.1016/j.ejmech.2022.114334>.
- [10] A. Gembarska, F. Luciani, C. Fedele, E.A. Russell, M. Dewaele, S. Villar, A. Zwolinska, S. Haupt, J. de Lange, D. Yip, J. Goydos, J.J. Haigh, Y. Haupt, L. Larue, A. Jochemsen, H. Shi, G. Moriceau, R.S. Lo, G. Ghanem, M. Shackleton, F. Bernal, J.C. Marine, MDM4 is a key therapeutic target in cutaneous melanoma, *Nat. Med.* 18 (2012) 1239–1247, <https://doi.org/10.1038/nm.2863>.
- [11] M. Espadinha, V. Barcherini, E.A. Lopes, M.M.M. Santos, An update on MDMX and dual MDM2/X inhibitors, *Curr. Top. Med. Chem.* 18 (2018) 647–660, <https://doi.org/10.2174/1568026618666180604080119>.
- [12] T. Franck, W.G. M., MDM2 and MDM4: p53 regulators as targets in anticancer therapy, *Int. J. Biochem. Cell Biol.* 39 (2007) 1476–1482, <https://doi.org/10.1016/j.biocel.2007.03.022>.
- [13] J. Kallen, A. Izaac, S. Chau, E. Wirth, J. Schoepfer, R. Mah, A. Schlapbach, S. Stutz, A. Vaupel, V. Guagnano, K. Masuya, T.-M. Stachyra, B. Salem, P. Chene, F. Gessier, P. Holzer, P. Furet, Structural states of Hdm2 and HdmX: X-ray elucidation of adaptations and binding interactions for different chemical compound classes, *ChemMedChem* 14 (2019) 1305–1314, <https://doi.org/10.1002/cmdc.201900201>.
- [14] A. Monteiro, L.M. Gonçalves, M.M. Santos, Synthesis of novel spiropyrazoline oxindoles and evaluation of cytotoxicity in cancer cell lines, *Eur. J. Med. Chem.* 79 (2014) 266–272, <https://doi.org/10.1016/j.ejmech.2014.04.023>.
- [15] R.C. Nunes, C.J.A. Ribeiro, A. Monteiro, C.M.P. Rodrigues, J.D. Amaral, M.M. Santos, In vitro targeting of colon cancer cells using spiropyrazoline oxindoles, *Eur. J. Med. Chem.* 139 (2017) 168–179, <https://doi.org/10.1016/j.ejmech.2017.07.057>.
- [16] J.D. Amaral, D. Silva, C.M.P. Rodrigues, S. Solá, M.M.M. Santos, A novel small molecule p53 stabilizer for brain cell differentiation, *Front. Chem.* 7 (2019), <https://doi.org/10.3389/fchem.2019.00015>.
- [17] C. Gomez, M. Gicquel, J.C. Carry, L. Schio, P. Retailleau, A. Voituriez, A. Marinetti, Phosphine-catalyzed synthesis of 3,3-spirocyclopenteneoxindoles from gamma-

- substituted allenoates: systematic studies and targeted applications, *J. Org. Chem.* 78 (2013) 1488–1496, <https://doi.org/10.1021/jo302460d>.
- [18] P.S. Dragovich, J.K. Blazel, K. Dao, D.A. Ellis, L.-S. Li, D.E. Murphy, F. Ruebsam, C. V. Tran, Y. Zhou, Regiospecific synthesis of novel 6-Amino-5-hydroxypyridazin-3 (2H)-ones, *Synthesis* (2008) 610–616, <https://doi.org/10.1055/s-2008-1032157>, 2008.
- [19] C.M. Hattinger, M.P. Patrizio, L. Fantoni, C. Casotti, C. Riganti, M. Serra, Drug resistance in osteosarcoma: emerging biomarkers, *Therapeutic Targets and Treatment Strategies*, *Cancers* 13 (2021) 2878, <https://doi.org/10.3390/cancers13122878>. Basel.
- [20] S.J. Shukla, R. Huang, C.P. Austin, M. Xia, The future of toxicity testing: a focus on in vitro methods using a quantitative high-throughput screening platform, *Drug Discov. Today* 15 (2010) 997–1007, <https://doi.org/10.1016/j.drudis.2010.07.007>.
- [21] S. Daniele, S. Taliani, E. Da Pozzo, C. Giacomelli, B. Costa, M.L. Trincavelli, L. Rossi, V. La Pietra, E. Barresi, A. Carotenuto, A. Limatola, A. Lamberti, L. Marinelli, E. Novellino, F. Da Settimo, C. Martini, Apoptosis therapy in cancer: the first single-molecule Co-activating p53 and the translocator protein in glioblastoma, *Sci. Rep.* 4 (2014) 4749, <https://doi.org/10.1038/srep04749>.
- [22] S. Daniele, E. Barresi, E. Zappelli, L. Marinelli, E. Novellino, F. Da Settimo, S. Taliani, M.L. Trincavelli, C. Martini, Long lasting MDM2/Translocator protein modulator: a new strategy for irreversible apoptosis of human glioblastoma cells, *Oncotarget* 7 (2016) 7866–7884, <https://doi.org/10.18632/oncotarget.6872>.
- [23] S. Daniele, V. La Pietra, E. Barresi, S. Di Maro, E. Da Pozzo, M. Robello, C. La Motta, S. Cosconati, S. Taliani, L. Marinelli, E. Novellino, C. Martini, F. Da Settimo, Lead optimization of 2-phenylindolyglyoxylyldipeptide murine double minute (MDM)2/Translocator protein (TSPO) dual inhibitors for the treatment of gliomas, *J. Med. Chem.* 59 (2016) 4526–4538, <https://doi.org/10.1021/acs.jmedchem.5b01767>.
- [24] S. Daniele, V. La Pietra, R. Piccarducci, D. Pietrobono, C. Cavallini, V.M. D'Amore, L. Cerofolini, S. Giuntini, P. Russomanno, M. Puxeddu, M. Nalli, M. Pedrini, M. Fragai, C. Luchinat, E. Novellino, S. Taliani, G. La Regina, R. Silvestri, C. Martini, L. Marinelli, CXCR4 antagonism sensitizes cancer cells to novel indole-based MDM2/4 inhibitors in glioblastoma multiforme, *Eur. J. Pharmacol.* 897 (2021), 173936, <https://doi.org/10.1016/j.ejphar.2021.173936>.
- [25] Y. Rew, D. Sun, X. Yan, H.P. Beck, J. Canon, A. Chen, J. Duquette, J. Eksterowicz, B.M. Fox, J. Fu, A.Z. Gonzalez, J. Houze, X. Huang, M. Jiang, L. Jin, Y. Li, Z. Li, Y. Ling, M.C. Lo, A.M. Long, L.R. McGee, J. McIntosh, J.D. Oliner, T. Osgood, A. Y. Saiki, P. Shaffer, Y.C. Wang, S. Wortman, P. Yakowec, Q. Ye, D. Yu, X. Zhao, J. Zhou, J.C. Medina, S.H. Olson, Discovery of AM-7209, a potent and selective 4-amidobenzoic acid inhibitor of the MDM2-p53 interaction, *J. Med. Chem.* 57 (2014) 10499–10511, <https://doi.org/10.1021/jm501550p>.
- [26] G.M. Popowicz, A. Czarna, S. Wolf, K. Wang, W. Wang, A. Dömling, T.A. Holak, Structures of low molecular weight inhibitors bound to MDMX and MDM2 reveal new approaches for p53-MDMX/MDM2 antagonist drug discovery, *Cell Cycle* 9 (2010) 1104–1111, <https://doi.org/10.4161/cc.9.6.10956>.
- [27] P.C. Hawkins, A. Nicholls, Conformer generation with OMEGA: learning from the data set and the analysis of failures, *J. Chem. Inf. Model.* 52 (2012) 2919–2936, <https://doi.org/10.1021/ci300314k>.
- [28] T.A. Halgren, Merck molecular force field. I. Basis, form, scope, parameterization, and performance of MMFF94, *J. Comput. Chem.* 17 (1996) 490–519, [https://doi.org/10.1002/\(SICI\)1096-987X\(199604\)17:5<490::AID-JCC1>3.0.CO;2-P](https://doi.org/10.1002/(SICI)1096-987X(199604)17:5<490::AID-JCC1>3.0.CO;2-P).
- [29] T.A. Halgren, V.I. Mmff, MMFF94s option for energy minimization studies, *Journal of Computational Chemistry* 20 (1999) 720–729, [https://doi.org/10.1002/\(SICI\)1096-987X\(199905\)20:7<720::AID-JCC7>3.0.CO;2-X](https://doi.org/10.1002/(SICI)1096-987X(199905)20:7<720::AID-JCC7>3.0.CO;2-X).
- [30] M. McGann, FRED pose prediction and virtual screening accuracy, *J. Chem. Inf. Model.* 51 (2011) 578–596, <https://doi.org/10.1021/ci100436p>.
- [31] C.C.G. Ulc, Molecular Operating Environment (MOE), in, 1010 Sherbooke St. West, Suite #910, 2022. Montreal, QC, Canada, H3A 2R7.
- [32] L. Schrödinger, The PyMOL Molecular Graphics System.
- [33] V. Zoete, M.A. Cuendet, A. Grosdidier, O. Michielin, SwissParam: a fast force field generation tool for small organic molecules, *J. Comput. Chem.* 32 (2011) 2359–2368, <https://doi.org/10.1002/jcc.21816>.
- [34] R. Kumari, R. Kumar, A. Lynn, g\_mmpbsa—a GROMACS tool for high-throughput MM-PBSA calculations, *J. Chem. Inf. Model.* 54 (2014) 1951–1962, <https://doi.org/10.1021/ci500020m>.